Sex, age, and regional differences in CHRM1 and CHRM3 genes expression levels in the human brain biopsies: potential targets for Alzheimer's disease-related sleep disturbances

Cristina Sanfilippo 1, Loretta Giuliano 2, Paola Castrogiovanni 3, Rosa Imbesi 3, Martina Ulivieri 4, Francesco Fazio 4, Kaj Blennow 5 6, Henrik Zetterberg 5 6 7 8, Michelino Di Rosa

Affiliations collapse

Affiliations

1IRCCS Centro Neurolesi Bonino Pulejo, Strada Statale 113, C.da Casazza, 98124 Messina, Italy.

2Department G.F. Ingrassia, Section of Neurosciences, University of Catania, Catania, Italy.

3Department of Biomedical and Biotechnological Sciences, Human Anatomy and Histology Section, School of Medicine, University of Catania, Italy.

4University of California San Diego, Department of Psychiatry, Health Science, San Diego La Jolla, CA, USA.

5Department of Psychiatry and Neurochemistry, Institute of Neuroscience and Physiology, Sahlgrenska Academy at the University of Gothenburg, Mölndal, Sweden.

6Clinical Neurochemistry Laboratory, Sahlgrenska University Hospital, Mölndal, Sweden.

7UK Dementia Research Institute at UCL, London, United Kingdom.

8Department of Neurodegenerative Disease, UCL Institute of Neurology, London, United Kingdom.

Abstract

Cholinergic hypofunction and sleep disturbance are hallmarks of Alzheimer's disease (AD), a progressive disorder leading to neuronal deterioration. Muscarinic acetylcholine receptor (M1-5 or mAChRs), expressed in hippocampus and cerebral cortex, play a pivotal role in the aberrant alterations of cognitive processing, memory, and learning, observed in AD. Recent evidence shows that two mAChRs, M1 and M3, encoded by CHRM1 and CHRM3 genes respectively, are involved in sleep functions, and, peculiarly, in the rapid eye movement (REM) sleep. We used twenty microarray datasets, extrapolated from post-mortem brain tissue of non-demented healthy controls (NDHC) and AD patients, to examine the expression profile of CHRM1 and CHRM3 genes. Samples were from eight brain regions and stratified according to age and sex. CHRM1 and CHRM3 expression levels were significantly reduced in AD compared with age- and sex-matched NDHC brains. A negative correlation with age emerged for both CHRM1 and CHRM3 in NDHC but not in AD brains. Notably, a marked positive correlation was also revealed between the neurogranin (NRGN) and both CHRM1 and CHRM3 genes. These associations were modulated by sex, accordingly in the temporal and occipital regions of NDHC subjects, males expressed higher levels of CHRM1 and CHRM3, respectively, than females. In AD patients, males expressed higher levels of CHRM1 and CHRM3 in the temporal and frontal regions, respectively, than females. Thus, substantial differences, all strictly linked to the brain region analyzed, age, and sex, exist in CHRM1 and CHRM3 brain levels both in NDHC subjects and in AD patients.

Keywords: Alzheimer’s disease; REM-Sleep; Sleep disturbance; Bioinformatics; CHRM1; CHRM3.

1. INTRODUCTION

Alzheimer's disease (AD) is the most common form of progressively disabling degenerative dementia in the elderly but there are also early-onset familial forms of the disease (Mayeux and

Stern, 2012). First described by Alois Alzheimer and his junior collaborator in 1910, Gaetano Perusini, since the description of the first case of Auguste Deter, the disease is characterized by severe cognitive deficits including memory loss and language impairment, leading to increasing dependence in everyday life (Gurwitz, 1997). However, even if there are psychiatric symptoms in AD, this disease is more commonly characterized as a neurodegenerative disorder, since its key pathological hallmarks include neuronal loss, and accumulation of amyloid β (Aβ) and tau proteins in plaques and tangles, respectively (Glenner and Wong, 1984; Grundke-Iqbal et al., 1986). There is also abundant evidence showing that activation of glial cells, including microglia and astrocytes, is an important part of the disease process and may contribute to low-grade neuroinflammation that may contribute to or prevent from neurodegeneration (Wang et al., 2015). Aβ plaques are responsible for the activation of glial cells (*i.e.*, microglia and astrocytes), thus inducing an immune response (El Khoury et al., 2003; Medeiros and LaFerla, 2013; Steardo et al., 2015), consequently considered fundamental for the formation of NFTs, and therefore contributing to neuronal dysfunction (Heppner et al., 2015).

The incidence of the disease is higher in women than in men; about two-thirds of people diagnosed with AD dementia are women. This cannot simply be attributed to the higher longevity of women versus men (Vina and Lloret, 2010), even if age is the greatest risk factor for AD dementia. As a result, and similar to other aging-related diseases, the lifetime risk of AD dementia is greater for women (Plassman et al., 2007). Even if women and men have the same incidence of AD dementia, the mechanisms, pathways, and risk factors can still differ. Many studies examining risk factors for AD 'adjust' for sex in their analysis, but they do not determine whether an actual sex difference exists. It has been shown that normal female microglia and estrogen have protective effects under normal conditions. However, under the influence of AD,

female microglia seem to lose their protective effect and instead accelerate the course of AD (Chen et al., 2021).

Neuroinflammation is considered a most relevant mechanism involved in almost all neurodegenerative diseases, including AD (Schain and Kreisl, 2017). Microglia and astrocytes are the main glial cells of the neuroimmune system, nevertheless, their interaction with the peripheral immune system is not yet clear (Kanegawa et al., 2016). Microglia are resident innate immunity cells that represent almost 10% of all the cells in the central nervous system (CNS) (Lawson et al., 1990). They are the first line of defense against invading pathogens or other types of brain debris discovered as non-self (Solito and Sastre, 2012). Microglia is endowed with both pro- and anti-inflammatory functions. In spite of their physiological role, proinflammatory activity could cause synaptic dysfunction and neuronal death (Schain and Kreisl, 2017). An imbalance between pro- and anti-inflammatory events could cause injury in the central nervous system and scientific evidence suggests that chronic low-level activation of glial cells could be a determinant factor in the pathogenesis of neurodegenerative disorders (Schain and Kreisl, 2017). Several studies have shown that microglia are involved in the formation of Aβ plaques in the brains of AD patients (Wyss-Coray and Rogers, 2012), and their involvement at the sites of Aβ deposition, suggest that these cells might physically interact with Aβ and regulate their levels in the brain (Cunningham et al., 2005). Astrocytes are the most abundant glial subtype in the brain, and similar to microglia cell, they play a relevant role in the modulation of neuroinflammation (Colombo and Farina, 2016). Structurally, these cells are close to blood vessels and interact with endothelial cells, actively participating in the maintenance and permeability of the blood-brain barrier (BBB) (Abbott, 2002). Recently, deep astrogliosis has been shown to be present in the brains of AD patients (Nagele et al., 2003). Analysis of AD patient brains has shown that reactive astrocytes accumulate around amyloid plaques where they phagocytose degenerated dendrites

and local synapses surrounding Aβ deposits (Wyss-Coray and Rogers, 2012). As a consequence of the presence of Aβ or following a signal of damage or injury, astrocytes intervene locally with the secretion of pro-inflammatory cytokines, which may contribute to the neurodegenerative processes typical of AD.

Among the proteins involved during neuroinflammation in AD, our attention focused on the family of chitinases, an ancient gene family including proteins, expressed in innate immune cells (Eide et al., 2016; Henrissat and Davies, 1997). In particular, chitotriosidase (CHIT1) and acidic mammalian chitinase (CHIA or AMCase) have a chitinolytic activities, instead chitinase-like-lectins (Chi-lectins) or chitinase-like proteins (C/CLPs), including chitinase 3-like-1 (CHI3L1, also called YKL40 or HC-gp39), chitinase 3-like-2 (CHI3L2) and chitinase domain containing 1 (CHID1 or SI-CLP), do not harbor the catalytic residues albeit with preservation of the substrate-binding cleft of the chitinases (Lee et al., 2011). The expression of chitinases is amplified during several infections, confirming, for these proteins, a likely part in inflammatory diseases and in innate immuno-activation (Di Rosa et al., 2016a; Di Rosa et al., 2016b). In relation to their function within the central nervous system (CNS), little is known of these proteins. CHI3L1 has been reported to be upregulated in a plethora of neurodegenerative disorders (Di Rosa et al., 2006; Harris and Sadiq, 2014; Varghese et al., 2013). Specifically, it has been associated with the pathogenesis of AD (Carter et al., 2019; Teitsdottir et al., 2021) and mainly expressed in astrocytes (Bonneh-Barkay et al., 2012). CHI3L1 expression levels are increased the nervous tissue of AD brains, as reported in our recent studies, leading us to hypothesize that CHI3L1 may have immunological activity in neuroinflammation (Di Rosa et al., 2006; Sanfilippo et al., 2016; Sanfilippo et al., 2019a; Sanfilippo et al., 2020a). CHI3L1 is considered a possible candidate biomarker of glial activation in AD when measured in cerebrospinal fluid (CSF), and several papers report a link among CHI3L1, neurodegeneration markers tau (Alcolea et al., 2014; Alcolea et al., 2015; Antonell et al., 2014;

Craig-Schapiro et al., 2010; Rehli et al., 2003), and neurofilament light (NFL) (Melah et al., 2016) in CSF (Querol-Vilaseca et al., 2017). In AD patients, CHI3L1 levels increase in CSF compared to non-demented healthy control subjects (NDHC) (Choi et al., 2011; Olsson et al., 2012; Rosen et al., 2014). Moreover, increased CHI3L1 levels in CSF have been recently detected also in macaques and humans with lentiviral encephalitis (Bonneh-Barkay et al., 2008). In our recent study, CHI3L1 was also related to dendritic cell activation and differentiation (Di Rosa et al., 2016b). In addition, CHI3L1 expression may be induced in astrocytes in traumatic brain injury (Bonneh-Barkay et al., 2010). Regards the chitinase-3-like protein 2 (CHI3L2 or YKL39) , this chitinase is a glycoprotein secreted by different cell types such as polarized macrophages (Di Rosa et al., 2013), dendritic cells (Di Rosa et al., 2016b), osteoclasts (Di Rosa et al., 2014b) and numerous cells with high proliferative activity (Qiu et al., 2018). Very little is known about the role of CHI3L2 (Litviakov et al., 2018). This chitinase-like protein is considered the closest homolog of CHI3L1 (Di Rosa et al., 2009; Di Rosa et al., 2014b). Its expression has been related to inflammatory pathogenesis. In recent years, different roles have been attributed to it, such as tissue remodeling during inflammation (Di Rosa and Malaguarnera, 2016), differentiation (Litviakov et al., 2018), and maturation of macrophages (Szychlinska et al., 2016). Its high levels have been associated with various pathological disorders, such as brain cancer (Di Rosa et al., 2015), diabetes (Di Rosa and Malaguarnera, 2016), osteoarthritis (Di Rosa et al., 2014a), asthma (Kwak et al., 2019), and HIV-1 infection (Sanfilippo et al., 2017b). CHI3L2 high expression levels have been detected in the brain of neurological disease such as neuro-HIV-1 (Sanfilippo et al., 2017b), amyotrophic lateral sclerosis (ALS) (Sanfilippo et al., 2017a), and AD (Sanfilippo et al., 2016; Sanfilippo et al., 2019a). Although CHI3L2 was initially associated with the macrophage lineage, evidence suggests that during neuroinflammatory processes, its expression is abundant in astrocytes (Wurm et al., 2019), microglial cells (Mollgaard et al., 2016) , and infiltrating macrophages (Litviakov et al., 2018;

Malaguarnera et al., 2005). Although its expression has been studied in different neuroinflammatory processes, to date there is no complete information on its possible correlation with markers of neuroimmune activation, alteration of the blood-brain barrier and neuronal transmission.

Here, we analyzed microarray datasets of brain samples from NDHC who died from causes not attributable to neurodegenerative diseases and from deceased patients suffering from AD. The significant transcriptomes, weighted according to CHI3L1 and CHI3L2 expression levels and sex, were therefore overlapped with the genes enriching CNS cells and Immune cells, aiming to discriminate the cellular architecture of AD patients' brains according to their sex.

2. MATERIALS AND METHODS

2.1 Dataset selection

The NCBI Gene Expression Omnibus (GEO) database (http://www.ncbi.nlm.nih.gov/geo/) (Clough and Barrett, 2016) was used to select transcriptomes datasets of interest. Mesh terms "Alzheimer", "brain", and "human", were used to identify the potential datasets to select. We sorted the datasets by the number of samples (High to Low), age, sex, and by the clinical data. Two datasets were selected, performed with the same platform (GPL4372), and subsequently merged for our analysis using z-score calculation (Statistical Analysis section) (Table 1). We chose to merge only the datasets with the same platform in order to reduce the errors oscillation introduced with different platforms. The datasets were selected following the criteria exposed in the section "Clinical and pathological criteria".

Table 1. Datasets selected

N°	Datasets	Organism	Samples	Platform	NDHC	AD	PMID
1	GSE44772	human	690	GPL4372	303 (246 ♂ and 57 ♀)	387 (186 ♂ and 201 ♀)	23622250

2	GSE33000	human	467	GPL4372	157 (123 ♂ and 34 ♀)	310 (135 ♂ and 175 ♀)	25080494
3	Merging	human	1157	GPL4372	460 (369 ♂ and 91 ♀)	697 (321 ♂ and 376 ♀)	//

Non-Demented Healthy Control subjects (**NDHC**); Alzheimer's Disease (**AD**)

2.2 Sample stratification

To test our hypotheses, we collected microarray datasets to gather brain samples of NDHC who died from causes not attributable to neurodegenerative diseases (n=460, 369 males, middle age (ma)=61.89, and 91 females, ma=65.45), and of deceased patients suffering from Alzheimer's disease (AD) (n=697, 321 males with ma=78.28, and 376 females with ma=82.11). The AD patients were selected according to sex and stratified using CHI3L1 and CHI3L2 expression levels as a cut-off. We obtained four groups subsequently used for our statistical comparisons. AD patients from the 75th percentile (upper quartile), were considered in this study as *High CHI3L1 expression group (HC1EG) and CHI3L2 expression group (HC2EG)*, which included 80 males patients (z-score= 0.87-> 3.20) and 94 females patients (z-score= 1.14-> 3.38) for CHI3L1, and 82 males patients (z-score= 0.53-> 4.00) and 95 females patients (z-score= 0.77-> 3.87) for CHI3L2. The *Low CHI3L1 expression group (LC1EG)* corresponded to the patients in the 25th percentile (lower quartile) and included 80 male patients (z-score= -0.43-> -1.67) and 94 female patients (z-score= -0.15-> -1.43). Furthermore, as regard the patients that express low levels of CHI3L2, we indicated as *Low CHI3L2 expression group (LC2EG) the* 25th percentile (lower quartile) and included 82 male patients (z-score= -0.44-> -1.84) and 97 female patients (z-score= -0.26-> -2.23).

Samples belonging to the 75th and 25th percentiles were interpreted as having a transcriptome that is concordant (significantly correlated) to the specified signature selected, and the values of the target gene expressed in the stratified samples as a function of the percentile values concordant with the expression of the gene chosen as specific signature (CHI3L1 and CHI3L2).

Furthermore, by stratifying the AD patients according to sex and then to CHI3L1 expression levels, as a subset signature, we found that, in males, 1365 unique genes (including CHI3L1) were significant positive correlated (GSPC) (r-range from 0.40 to 0.83) and 1455 unique genes significant negative correlated (GSNC) (r-range from -0.40 to -0.66) to CHI3L1 expression levels (Supplementary Table 1) (Table 2). As regard the female's group, we found that there were 2323 unique GSPC (r-range from 0.40 to 0.84) and 816 unique GSNC (r-range from -0.40 to -0.61) to CHI3L1 expression levels (Supplementary Table 1) (Table 2). As regards CHI3L2, we found that, in males, 2113 unique genes (including CHI3L2) were significant positive correlated (GSPC) (r-range from 0.40 to 0.81) and 1502 unique genes significant negative correlated (GSNC) (r-range from -0.40 to -0.66) to CHI3L2 expression levels (Supplementary Table 1) (Table 2). As regard the female's group, we found that there were 3313 unique GSPC (r-range from 0.40 to 0.86) and 3049 unique GSNC (r-range from -0.40 to -0.67) to CHI3L2 expression levels (Supplementary Table 1) (Table 2).

Table 2: AD patients' stratification

SAMPLES	**MALES**	**FEMALES**
High CHI3L1 expression group (HCEG1) (75th percentile)	80	94
High CHI3L2 expression group (HCEG2) (75th percentile)	82	95
Low CHI3L1 expression group (LCEG1) (25th percentile)	80	94
Low CHI3L2 expression group (LCEG2) (25th percentile)	82	97
z-score value cut-off *(75th percentile) for CHI3L1*	0.87-> 3.20	1.14-> 3.38
z-score value cut-off *(75th percentile) for CHI3L2*	0.53-> 4.00	0.77-> 3.87
z-score value cut-off *(25th percentile) for CHI3L1*	-0.43-> -1.67	-0.15-> -1.43
z-score value cut-off *(25th percentile) forCHI3L2*	-0.44-> -1.84	-0.26-> -2.23
Middle age *(75th percentile) for CHI3L1*	78.32	83.48
Middle age *(75th percentile) for CHI3L2*	78.10	84
Middle age *(25th percentile) for CHI3L1*	75.95	81.57
Middle age *(25th percentile) for CHI3L2*	74.98	78.82
Unique Genes significant positive correlated (GSPC1) to CHI3L1	2314 (r=0.30->0.83)	2338 (r=0.30->0.84)
Unique Genes significant positive correlated (GSPC2) to CHI3L2	1847 (r=0.30->0.81)	2909 (r=0.30->0.86)
Unique Genes significant negative correlated (GSNC1) to CHI3L1	2020 (r=-0.30->-0.61)	1380 (r=-0.30->-0.61)

Unique Genes significant negative correlated (GSNC2) to CHI3L2	1406 (r=-0.30->-0.66)	2806 (r=-0.30->-0.67)

Besides, we excluded common genes attained by through overlapping between males positive/negative and females positive/negative AD correlated to CHI3L1 and CHI3L2, respectively (Supplementary Table 1).

2.3 Clinical and pathological criteria

Most of the samples analyzed were obtained from public tissue banks (Table1). Sample pH, and RNA integrity number (RIN) were elements of pre-selection by the authors of the reference microarray datasets, and subsequently, object of our further exclusion analysis. The authors of original studies reported that all patients gave informed consent, and this study was approved by the medical ethics committees of all sites. All specimens were derived from brain biopsies and were snap-frozen in liquid nitrogen immediately after surgery for storage at –80°C.

2.4 Data processing and experimental design

To process and identify Significantly Different Expressed Genes (SDEG) within the datasets, we used the MultiExperiment Viewer (MeV) software (The Institute for Genomic Research (TIGR), J. Craig Venter Institute, La Jolla, USA). In cases where multiple genes probes have insisted on the same GeneID NCBI, we used those with the highest variance.

With the aim of identifying genes commonly modulated between the GSE datasets present in Table 1 and cell type-specific genes for brain cells, we performed a Venn diagram analysis, using the web-based utility Venn Diagram Generator (http://bioinformatics.psb.ugent.be/webtools/Venn/) (Castrogiovanni et al., 2018; Sanfilippo et al., 2019b). For GSE44772 and GSE33000 we also performed a statistical analysis with GEO2R,

applying a Benjamini-Hochberg false discovery rate test (Davis and Meltzer, 2007; Smyth, 2004; Xiao et al., 2017).

Gene ontology (GO) analysis was performed using the web utility GeneMANIA (http://genemania.org/) (Zuberi et al., 2013), STRING (https://string-db.org/) (Szklarczyk et al., 2019), and the GATHER (Gene Annotation Tool to Help Explain Relationships) (http://changlab.uth.tmc.edu/gather/) (Chang and Nevins, 2006). The STRING was also used for building the weighted gene networks commonly modulated, rendered by CorelDRAW2020 (Corel Corporation, Ottawa, Ontario, Canada).

Additionally, we used public human brain single-cell RNA-sequencing data (RNA-seq, accession no. GSE67835) in order to carry out a panel of cell tissue-specific genes for five main brain cells, i.e. astrocytes (n=191), endothelial cells (endotheliocytes) (n=76), neurons (n=1032), microglia (n=118), and oligodendrocytes (n=111) (Wang et al., 2016). From GSE46236, we sorted the SDEG of pericyte immune-activated (n=333)(Guijarro-Munoz et al., 2014).

Furthermore, we decided to deepen the analysis including the immune system cellular profiles, consisting of CD8 T cell (naïve and resting) (CTLs) (n=63), classical Natural Killer (NK) (n=125), T helper cell type 1 (Th1) (n=221) and 2 (Th2) (n=98), obtained from the GSE22886 and two population of macrophages classical and alternative activated, macrophages M1 (n=823) and macrophages M2 (n=160) from GSE5099. As regard the immune-cells GSE22886 dataset, was composed by isolated twelve different types of human leukocytes from peripheral blood and bone marrow. In order to obtain the genes characterizing these cells, we have excluded all significant genes overlapped between all types of human leukocytes and successively, we selected only genes mutually exclusively significant up-regulated (Abbas et al., 2005; Sanfilippo et al., 2019b).

2.5 Statistical analysis

For statistical analysis, Prism 9 software (GraphPad Software, La Jolla, CA, USA) was used (Giunta et al., 2015). Statistical significance of the overlap between two groups of genes was calculated with Exact hypergeometric probability. The representation factor shows whether genes from one list (list A) are enriched in another list (list B), assuming that genes behave independently. The representation factor is defined as: (number of genes in common between both lists) (number of genes in the genome)/(number of genes in list A)(number of genes in list B). A RF > 1 indicates more overlap than expected between the two independent groups, a RF < 1 indicates less overlap than expected, and a RF of 1 indicates that the two groups are identical by the number of genes expected to be independent in the groups.

$$\text{The representation factor} = x \,/\, \text{expected \# of genes.}$$

$$\text{Expected \# of genes} = (n * D) / N$$

The probability of finding x overlapping genes can be calculated using the hypergeometric probability formula:

$$C(D, x) * C(N\text{-}D, n\text{-}x) / C(N,n)$$

where x = # of genes in common between two groups; n = # of genes in group 1; D = # of genes in group 2; N = total genes, in this case 20203 genes (RefSeq, a database run by the US National Center for Biotechnology Information (NCBI)); C (a,b) is the number of combinations of a thing taken 'b' at 'a' time (Buchman et al., 2012; Hillman et al., 2008).

Significant differences between groups were assessed using the Ordinary one-way ANOVA test, and Tukey's multiple comparisons test correction was executed to compare data among all groups. Correlations were determined using Pearson correlation. All tests were two-sided and significance was determined at adjusted p value 0.05. All datasets selected were transformed for

the analysis in Z-score intensity signal. Z score was constructed by taking the ratio of weighted mean difference and combined standard deviation according to Box and Tiao (1992) (Tiao, 6 April 1992). The application of a classical method of data normalization, z-score transformation, provides a way of standardizing data across a wide range of experiments and allows the comparison of microarray data independent of the original hybridization intensities. The z-score it is considered a reliable procedure for this type of analysis and can be considered a state-of-the-art methods, as demonstrated by the numerous bibliography (Care et al., 2013; Cheadle et al., 2003a; Cheadle et al., 2003b; Chen et al., 2008; Feng et al., 2018; Kang et al., 2019; Le Cao et al., 2014; Mehmood et al., 2017; Reddy et al., 2009; Wang et al., 2004; Yasrebi et al., 2009).

The efficiency of each biomarker was assessed by the receiver operating characteristic (ROC) curve analyses. Nonparametric ROC curves analyzed AD vs NDHC. The area under the ROC curve (AUC) and its 95% confidence interval (95% CI) indicates diagnostic efficiency. The accuracy of the test with the percent error is reported (Zetterberg et al., 2019).

3. Results

3.1 CHI3L1 and CHI3L2 expression in AD compared with non-AD brain tissue

Aiming to analyze CHI3L1 and CHI3L2 expression levels in AD brains, we merged microarray datasets with the same platform after transformation into z-scores. We obtained data from 460 NDHC brains (369 males and 91 females), and 687 AD brains (321 males and 376 females) (Table 1). Expression analysis revealed a significant increase in CHI3L1 and CHI3L2 levels in AD compared with non-AD brains ($p<0.0001$) (Figure 1a). To evaluate the potential diagnostic ability of CHI3L1 and CHI3L2 to discriminate between AD patients and NDHC subjects, we applied a receiver operating characteristic (ROC) analysis. CHI3L1 expressed an excellent diagnostic ability to discriminate AD from NDHC brains (AUC = 0.8570, $p < 0.0001$), and CHI3L2 showed satisfactory

performance ($p<0.0001$, AUC=0.6932) (Figure 1b). Since chitinases are closely linked to the aging process, we correlated CHI3L1 and CHI3L2 expression with age in AD and non-AD subjects. The Pearson correlation analysis performed highlighted high significant correlation between CHI3L1 ($r = 0.4743$, $p <0.0001$), and CHI3L2 ($r = 0.3523$, $p <0.0001$), and age (Supplementary Figure 1). To verify the close relationship between chitinases and astroglia, and microglia cells, we performed correlation analysis with the GFAP as astroglia marker (Zhang et al., 2019), and with TMEM119 as microglia marker (Kenkhuis et al., 2022; Satoh et al., 2016). The analysis showed significant positive correlation between CHI3L1 ($r = 0.3566$, $p <0.0001$), CHI3L2 ($r = 0.4479$, $p <0.0001$), and GFAP expression levels in AD brain biopsies (Figure 1c). Furthermore, we highlighted significant positive correlation between CHI3L1 ($r = 0.2845$, $p <0.0001$), and CHI3L2 ($r = 0.1471$, $p <0.0001$), and TMEM119 expression levels in AD brain biopsies (Figure 1d).

By stratifying the samples according to sex, we found significant variations in the expression levels of the two chitinases. Indeed, both the expression levels of CHI3L1 ($p <0.001$) and those of CHI3L2 ($p <0.001$) were significantly higher in AD females than in males compared with NDHC subjects, and the AD females expressed significant higher levels of CHI3L1 compared to CHI3L2 ($p<0.001$) (Figure 2a). Furthermore, the brain expression levels of the two chitinases were positively correlated with each other in AD patients ($r = 0.5248$, $p <0.0001$) (Figure 2b), and this correlation remained significant in both males ($r = 0.4639$, $p <0.0001$) (Figure 2c) than in AD females ($r = 0.5495$, $p <0.0001$) (Figure 2d), albeit with a slight slope of the curve in males compared to females ($r = 0.4639$ in males, $r = 0.5495$ in females). All these findings are in accordance with data previously reported by our group (Castrogiovanni et al., 2021; Di Rosa et al., 2006; Malaguarnera et al., 2006; Motta et al., 2007; Sanfilippo et al., 2016; Sanfilippo et al., 2019a; Sanfilippo et al., 2020a; Sanfilippo et al., 2020b).

3.2 AD males and females exhibit different brain neuro-immune cellular profile according to CHI3L1 and CHI3L2 expression levels

We conducted a genomic deconvolution analysis (GDA) using neuro-immune signatures (NIS) obtained from GEODatasets, KEGG, and AmiGo (Table 3). Cell signatures covered six neurological and six immune cells populations, as described in the Materials and Methods section.

Table 3: The twelve signature – Neuro-immune signature (NIS)

N°	CELLS AND PROCESSES	SOURCE	UNIQUE GENES
1	Astrocyte	GSE67835	177
2	Endothelial cells	GSE67835	55
3	Microglia	GSE67835	93
4	Neuron	GSE67835	974
5	Oligodendrocytes	GSE67835	95
6	Pericyte immune activated	GSE46236	206
7	CTLs	GSE22886	58
8	M_1 macrophages	GSE5099	674
9	M_2 macrophages	GSE5099	132
10	Natural Killer (NK)	GSE22886	114
11	Th_1	GSE22886	191
12	Th_2	GSE22886	85

The NIS were overlapped to 2314 and 1847 genes significantly positively correlated respectively to CHI3L1 and CHI3L2 expression levels in AD males' brains (GSPC-CHI3L1-males, and GSPC-CHI3L2-males) (Figure 3a). Furthermore, we overlapped the NIS to 2338 and 2909 genes significantly positively correlated respectively to CHI3L1 and CHI3L2 expression levels in AD females' brains (GSPC-CHI3L1-females, and GSPC-CHI3L2-females) ($r>0.40$, strong positive relationship) (Supplementary Table 1).

The analysis showed that genes related to the expression of the two chitinases delineated similar brain cell profiles in AD males (Figure 3a), and females (Figure 3b). Specifically, as regards the GSPC-CHI3L1-males significant overlapped were highlighted for the cellular signatures of the astrocyte (ngene = 69, n%= 38.98, neglog10(pvalue) = 20.60, RF = 3.40), endothelial cells (ngene = 31, n%= 56.36, neglog10(pvalue) = 15.06, RF = 4.92), microglia (ngene = 63, n%= 67.74,

neglog10(pvalue) = 36.79, RF = 5.91), pericyte inflammatory (ngene = 46, n%= 22.33, neglog10(pvalue) = 5.21, RF = 1.94), M1 macrophages (ngene = 175, n%= 25.96, neglog10 (pvalue) = 25.73, RF = 2.26), and M2 macrophages (ngene = 35, n%= 26.51, neglog10(pvalue) = 5.86, RF = 2.31) (Figure 3a). Regarding the excluded NIS, such as neurons, oligodendrocytes, CTLs, natural killer (NK), Th1, and Th2 cells, the RF value was <1, so the intersections differed significantly from the individual processes (Supplementary Table 1) (Figure 3a).

The NIS also overlapped to the GSPC-CHI3L2-males (Figure 3a). The intersection highlighted significant overlaps with signatures of astrocyte (ngene = 52, n%= 21.37, neglog10(pvalue) = 13.92, RF = 3.21), endothelial cells (ngene = 16, n%= 29.09, neglog10(pvalue) = 4.68, RF = 3.18), microglia (ngene = 56, n%= 60.21, neglog10(pvalue) = 33.92, RF = 6.59), pericyte inflammatory (ngene = 35, n%= 16.99, neglog10(pvalue) = 3.60, RF = 1.85), M1 macrophages (ngene = 147, n%= 21.81, neglog10(pvalue) = 23.38, RF = 2.38), and M2 macrophages (ngene = 21, n%= 15.90, neglog10(pvalue) = 2.06, RF = 1.74) (Supplementary Table 1) (Figure 3a). For the NIS belonging to neurons, oligodendrocytes, CTLs, NK, Th1, and Th2 cells, the RF value was <1, so the intersections differed significantly from the individual processes (Supplementary Table 1) (Figure 3a).

In GSPC-CHI3L1-females, significant overlaps were highlighted for the NIS profiles belonging to the astrocytes (ngene = 31, n%= 17.51, neglog10(pvalue) = 1.91, RF = 1.51), endothelial cells (ngene = 23, n%= 41.81, neglog10(pvalue) = 7.92, RF = 3.61), microglia (ngene = 65, n%= 69.98, neglog10(pvalue) = 38.99, RF = 6.03), pericyte inflammatory (ngene = 47, n%= 22.81, neglog10(pvalue) = 5.46, RF = 1.97), M1 macrophages (ngene = 194, n%= 28.78, neglog10(pvalue) = 34.42, RF = 2.48), and M2 macrophages (ngene = 30, n%= 22.72, neglog10(pvalue) = 3.69, RF = 1.96) (Figure 3b). Regarding the excluded NIS, such as neurons, oligodendrocytes, CTLs, NK, Th1, and Th2 cells, the RF value was <1, so the intersections differed significantly from the individual processes (Supplementary Table 1) (Figure 3b).

Since GSPC-CHI3L2-females overlapped to the NIS, we highlighted significant overlaps with astrocytes (ngene = 42, n%= 23.72, neglog10(pvalue) = 3.21, RF = 1.65), endothelial cells (ngene = 20, n%= 36.36, neglog10(pvalue) = 4.36, RF = 2.52), microglia (ngene = 58, n%= 62.36, neglog10(pvalue) = 25.63, RF = 4.33), oligodendrocytes (ngene = 23, n%= 24.21, neglog10(pvalue) = 2.12, RF = 1.68), pericyte inflammatory (ngene = 40, n%= 19.11, neglog10(pvalue) = 1.55, RF = 1.34), and M1 macrophages (ngene = 195, n%= 28.93, neglog10(pvalue) = 22.52, RF = 2.01) (Supplementary Table 1) (Figure 3b). Regarding the excluded NIS, such as neurons, CTLs, NK, Th1, and Th2 cells, the RF value was <1, so the intersections differed significantly from the individual processes (Figure 3b).

The NIS were also overlapped to 2020 and 1406 genes that were negatively correlated with CHI3L1 and CHI3L2 expression levels in AD males' brains (GSNC-CHI3L1-males, and GSNC-CHI3L2-males) (Figure 4a). Furthermore, we overlapped the NIS to 1380 and 2806 genes significantly negatively correlated respectively to CHI3L1 and CHI3L2 expression levels in AD females' brains (GSNC-CHI3L1-females, and GSNC-CHI3L2-females) (r>0.40, strong positive relationship) (Supplementary Table 1).

The analysis showed that genes related to the expression of the two chitinases delineated similar brain expression profiles in AD males (Figure 4a) and females (Figure 4b). Specifically, as regards the GSNC-CHI3L1-males significant overlaps were highlighted only for the neuronal signatures (ngene = 277, n%= 28.43, neglog10(pvalue) = 61.90, RF = 2.84). Similar results were obtained for GSNC-CHI3L2-males (ngene = 282, n%= 28.95, neglog10(pvalue) = 103.40, RF = 4.16). Regarding the remaining NIS excluded, the RF value was <1, so the intersections differed significantly from the individual processes (Supplementary Table 1) (Figure 4a).

Regarding female profiles, we showed that genes related to the expression of the two chitinases delineated similar NIS such as in the AD males (Figure 4b). Specifically, as regards the GSNC-

CHI3L1-females, significative overlapped were highlighted only for the neuron cellular signatures (ngene = 134, n%= 13.75, neglog10(pvalue) = 14.55, RF = 2.01). In GSNC-CHI3L2-females, similar results were obtained (ngene = 425, n%= 43.63, neglog10(pvalue) = 119.90, RF = 3.14). Regarding the remaining NIS excluded, the RF value was <1, so the intersections differed significantly from the individual processes (Supplementary Table 1) (Figure 4b).

All these findings highlight the significant overlap between GS(P/N) C-CHI3L1 and GS(P/N)C-CHI3L2 and microglia, astrocyte, endothelial cells, pericyte inflammatory, and neuron NIS (Figure 5).

3.3 Signature similarity between CHI3L1 and CHI3L2 cellular profiles

We decided to overlap the genes belonging to the NIS defined by the GSPC-CHI3L1/CHI3L2, and GSNC-CHI3L1/CHI3L2 to identify the percentage similarity between the two chitinases (Table 4).

Table 4: Signature similarity

		MALE		**FEMALE**	
profiles	*neuro-immune signature*	***CHI3L1***	***CHI3L2***	***CHI3L1***	***CHI3L2***
GSPC	astrocyte	52.2	69.2	61.3	45.2
	endothelial cells	51.6	94.1	73.9	85.0
	microglia	87.3	98.2	86.2	96.6
	pericyte inflammatory	63.0	82.9	70.2	82.5
	M1 macrophages	72.6	86.4	77.3	76.9
	M2 macrophages	42.9	71.4	56.7	65.4
GSNC	neuron	44.8	44.0	83.6	26.4

Our analysis showed that the NIS significantly regulated by GSPC-CHI3L2 in both males and females AD were largely contained in those determined by GSPC-CHI3L1 (Table 4). In particular, when we compared the male profiles, the percentages of genes involved were higher for the NIS determined by GSPC-CHI3L1 (67.74% microglia) (Figure 6a) (Supplementary Table 1).

Furthermore, the signature of the microglia identified by the GSPC-CHI3L2-male showed the highest percentage of transcriptomic similarity to GSPC-CHI3L2-male (98.2%), while the lowest transcriptomic similarity was due to the M2 macrophages identified by the GSPC-CHI3L1-male signature (42.9%) (Table 4) (Supplementary Table 1) (Figure 6b, c). Also, for the female profiles we showed higher percentages of genes belonging to NIS significantly regulated by GSPC-CHI3L1 (microglia 68.89%) (Figure 7a) (Supplementary Table 1). Regarding the signature similarity between the profiles identified by the two chitinases, the signature of the microglia identified by the GSPC-CHI3L2-female showed the highest percentage of transcriptomic similarity to the GSPC-CHI3L1-female (96.6%), while the signature of the astrocytes identified from GSPC-CHI3L2-female showed the lowest transcriptomic similarity (45.2%) (Table 4) (Figure 7b, c) (Supplementary Table 1).

Regarding the NIS highlighted by GSNC-CHI3L1 and GSNC-CHI3L2 in both AD males and females, they showed data only significant for neuron signatures (Figure 8) (Table 4). In particular, when we compared the male and female profiles identified by the two chitinases, the percentages of the genes involved were higher in the NIS determined by GSNC-CHI3L2 (28.95% for the male, and 43.63% for the female) (Figure 8a) (Supplementary Table 1). Furthermore, the signature similarity of neurons identified by GNPC-CHI3L1-female showed the highest percentage of transcriptomic similarity to GSNC-CHI3L2-female (83.6%), while the signature similarities of male neurons were almost identical (44.8% for the CHI3L1-male, and 44.0 for the CHI3L2-male) (Table 4) (Figure 8b, c).

3.4 Biological processes identified by the common genes between the microglia, and neuron signatures determined by CHI3L1 and CHI3L2

Having emerged from our results that the microglia and neuron signatures were the most regulated by CHI3L1 and CHI3L2, we decided to verify the genes in common between GSPC-

CHI3L1/2-male/female for microglia, and GSNC-CHI3L1/2-male-female for neurons. We performed a Venn's analysis by crossing the microglia NIS signatures obtained from the GSPC-CHI3L1-male, GSPC-CHI3L1-female, GSPC-CHI3L2-male, and GSPC-CHI3L2-female data sets. The analysis showed 50 genes in common between all microglia-NIS. Regarding the 50 genes in common, the largest percentage contribution was that shared by microglia-CHI3L2-male (89%) (76% for microglia-CHI3L1-male, 86% for microglia-CHI3L2-female, and 79% for microglia-CH3L1-female) (Figure 9a) (Supplementary Table 1). Furthermore, we performed a GO analysis of the 50 genes in common among the microglia-NIS (Figure 9b). The data showed that the 66% (33 genes) were involved in biological processes of immune response (FDR = 4.30E-20, n = 33) (Figure 9b) (Supplementary Table 1). Other processes, such as leukocyte chemotaxis (FDR = 1.47E-05, n = 7), leukocyte migration (FDR = 0.00016, n = 8), positive regulation of chemotaxis (FDR = 0.00025, n = 6), and neutrophil chemotaxis (FDR = 0.0031, n = 4), were significantly activated by the signature of the 50 genes.

Regarding the neuron-NIS obtained with the overlapping of GSNC-CHI3L1-male, GSNC-CHI3L1-female, GSNC-CHI3L2-male, and GSNC-CHI3L2-female, Venn's analysis showed 32 genes in common between all neurons-NIS (Figure 9c) (Supplementary Table 1). Noteworthy, regarding the 32 genes in common, the largest percentage contribution was that shared by neuron-CHI3L1-female (23%) (7.5% for neuron-CHI3L2-female, 11.3% for neuron-CHI3L2-male, and 11.5% for neuron-CH3L1-male) (Figure 9c) (Supplementary Table 1). GO analysis of the 32 genes in common between neuron-NIS (Figure 9d) showed that 18% (5 genes) were involved in biological processes of regulation of neurotransmitter secretion (FDR = 0.001, n = 5) (Figures 9d) (Supplementary Table 1). Another significantly modulated process was the positive regulation of dendrite extension (FDR = 0.034, n = 3) (Supplementary Table 1).

4. Discussion

In recent years, the use of datasets available in public databases has grown exponentially. Different research groups have extensively used the analysis of public transcriptome datasets for the identification of novel pathogenic pathways and therapeutic targets in a number of human pathologies (Catrogiovanni et al., 2020; Sanfilippo et al., 2017b; Sanfilippo et al., 2018), including neurodegenerative diseases (Castrogiovanni et al., 2018; Sanfilippo et al., 2016; Sanfilippo et al., 2017b; Sanfilippo et al., 2019b) and cancer (Di Rosa et al., 2015; Di Rosa et al., 2020). Through a meta-analysis of public transcriptome datasets, it is possible to increase the statistical power to obtain a more precise estimation of gene expression differentials and assess the heterogeneity of the overall estimation. Meta-analysis is relatively inexpensive since it makes comprehensive use of already available data and represents a vast source of information that could make a difference in setting up highly targeted experimental strategies.

Elevated levels of chitin have been found in CNS, CSF, and plasma in AD patients. Furthermore, this polymer has been implicated in influencing Aβ accumulation and AD pathogenesis (Lomiguen et al., 2018). The involvement of chitinases in immune-mediated degenerative processes is currently a hot topic. There are wide studies on CHI3L1 as cerebrospinal fluid biomarker that increases with aging and early in AD, much less so regarding CHI3L2 (Hong et al., 2021). Currently, the two chitinases at the CNS level are considered purely astrocytic proteins, but a strong microglial regulation emerges from our results. The purpose of our analysis it has been to profile the AD patient's brains according to the CHI3L1 and CHI3L2 expression levels, and subsequently highlight AD-NIS sex-depended. Our analysis showed a significant increase in CHI3L1 and CHI3L2 expression levels in AD patients compared to NDHC subjects. These data are closely aligned with our previous results and with bibliographic data from other research groups that have demonstrated variation in expression levels in AD CSF (Hong et al., 2021). Specifically,

our group confirmed the presence of CHI3L1, CHI3L2, CHID1, and CHIT1 in the brains of AD patients, also demonstrating for the first time a sex-linked difference in CHI3L1 and CHI3L2 expression levels. Recently, we showed a positive correlation between CHI3L2 and the microglia-mediated neuroinflammation (IBA1), alteration of the blood-brain barrier (PECAM1), and neuronal damage (CALB1) expression levels, further demonstrating the positive correlation that exists between CHI3L2 and its homolog CHI3L1 (Sanfilippo et al., 2020a). Furthermore, expression analysis of another chitinase, CHID1, showed diametrically opposite behavior to CHI3L1 and CHI3L2. Indeed, the CHID1 expression levels in the brains of AD patients were positively correlated with CALB1 and neurogranin (NRGN), demonstrating a function closer to neurons than to astrocytes/microglia/endothelial cells, typical of CHI3L1 and CHI3L2 (Castrogiovanni et al., 2021).

Interestingly, the expression levels of the two chitinases had a higher r Pearson index for GFAP than for TMEM119, as well as r Pearson index higher for CHI3L2 compared with CHI3L1. This finding further supports the hypothesis that CHI3L1, and its homolog CHI3L2, are typically astroglial proteins whose function is expressed on target cells such as microglia (Connolly et al., 2022).

Recently, it has been shown that CHI3L1 is not only expressed in astrocytes, but also in reactive and neurotoxic astrocytes, which are induced by microglia (Clarke et al., 2018). It can also regulate microglial activation states that may induce neuronal death (Connolly et al., 2022). Indeed, we showed NIS overlap between those identified by GS(P/N) C-CHI3L1 and GS(P/N)C-CHI3L2, particularly striking in microglia, astrocyte, endothelial cells, pericyte inflammatory, M1 macrophages, and neuron signatures. On the one hand, the GSPCs to CHI3L1 and CHI3L2 characterize astrocytic cells, on the other hand, they could have microglia, inflammatory pericytes, M1 macrophages, and endothelial cells as activation targets. Our data demonstrate

that CHI3L1 and CHI3L2 could modulate the expression and secretion of proinflammatory cytokines from glial cells, resulting in BBB disruption (Supplementary Table 1). CHI3L1 has been shown to be involved in BBB disruption and remodeling of the blood vasculature in AD, confirming the modulation of endothelial cells and pericytes highlighted by our results (Moreno-Rodriguez et al., 2020). Furthermore, in our analysis, we showed that the percentage of similarity between microglial and neuronal signatures showed that the microglial transcripts identified by positively correlated to CHI3L2 (microglia-CHI3L2) were almost completely contained in that identified by CHI3L1 (microglia-CHI3L1), both in male and female AD patients, suggesting a similar role played by the two chitinases at the level of AD microglia regulation. It has been shown that CHI3L1 plays a direct role in neurons. This effect can potentially be related to synapse loss, as well as the accumulation of misfolded proteins and the appearance of well-defined neurodegenerative features prior to overt plaque and tangle formation (Liddelow and Barres, 2017). When we analyzed the NIS highlighted by the signatures negatively correlated with the expression of CHI3L1 and CHI3L2, we found significant data only for neurons. Furthermore, when we measured the percent degree of overlap, we found that those identified by the female signature of CHI3L1 (neuron-CHI3L1-female) were contained in that of CHI3L2 (neuron-CHI3L2-female), suggesting a more prominent neuronal role for the negatively related genes of CHI3L2.

The analysis of our results allows us to hypothesize that CHI3L1 and CHI3L2 function as neuronal cytokines that mediate neuroinflammatory processes in order to trigger receptors expressed on target brain cells (astrocyte, microglia, pericytes, endothelial cells, and M1) and regulate innate inflammatory responses. In this way, CHI3L1 and CHI3L2 would play an essential role in the communication dynamics between microglia and astrocytes in the process of neuroinflammation. Furthermore, the action on endothelial cells and pericytes could contribute to the compromise of the integrity of the BBB, a process also observed in AD patients. Yet

another effect potentially played by CHI3L1 and CHI3L2 could be the direct one on neurons, which we highlighted indirectly, in which cell death phenomena linked to the loss of synapses would be triggered as well as the accumulation of misfolded proteins and the appearance of well-defined neurodegenerative characteristics before the overt formation of plaques and tangles. All these findings led us to hypothesize that the two chitinases, CHI3L1 and CHI3L2, play a potentially similar role in the brains of AD patients (Figure 10).

Conclusion

Our investigations revealed the similarities identified in AD brains based on the expression levels of CHI3L1 and CHI3L2, suggesting a similar role played by the two chitinases. These similarities would suggest an increase in the regulatory activity of microglia, pericytes, and endothelial cells by astrocytes through the use of the two chitinases. Further studies will be needed to concretely corroborate the neuroinflammatory role played by CHI3L1 and CHI3L2 in the human brain. Being able to characterize the signal transduction mechanisms operated by CHI3L1 and CHI3L2 on CNS cells leading to neuroinflammation could provide new opportunities for the development of new drugs necessary for the treatment of patients with AD or affected by other neurodegenerative diseases.

Acknowledgements

We would like to show our gratitude to the authors of microarray datasets made available online, for consultation and re-analysis. We would like to thank Led Zeppelin for inspiring us to write this manuscript.

Declarations

Competing interests

The authors declare no competing interests.

Consent to publish

Not applicable

Consent to participate

Not applicable

Ethics approval

Not applicable. The ethics approval and consent to participate were requested by the authors of the original datasets shown in Table 1, and subsequently analyzed in our study.

Data availability

The datasets analysed during the current study are available in the GEODaset repository, Home - GEO DataSets - NCBI (nih.gov).

Authors' contribution statements

The study was conceptualized and designed by Michelino Di Rosa. The original manuscript was written by Michelino Di Rosa, Cristina Sanfilippo, Paola Castrogiovanni, and Francesco Fazio. Data curation, were performed by Michele Vecchio, Giovanni Li Volti, Daniele Tibullo, Giuseppe Musumeci, Martina Ulivieri, Francesco Fazio, Maria Kazakova, Rosa Imbesi. Methodology and formal analysis were performed by Cristina Sanfilippo, and Paola Castrogiovanni. The manuscript was revised and improved by Michelino Di Rosa.

Funding/Support

This study was supported by the University Research Project Grant (PIACERI 2020–2022), Department of Biomedical and Biotechnological Sciences (BIOMETEC), University of Catania, Italy. The funder/sponsor had no role in the design and conduct of the study; collection, management, analysis, and interpretation of the data; preparation, review, or approval of the manuscript; and decision to submit the manuscript for publication. HZ is a Wallenberg Scholar.

Figures Legends

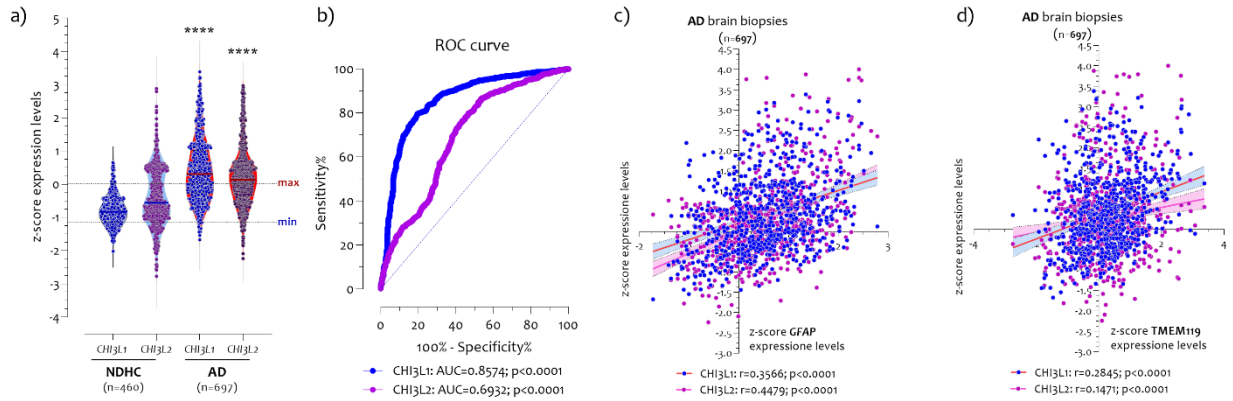

Figure 1: CHI3L1 and Chi3L2 expression levels in AD brains

Significant increase of CHI3L1 and Chi3L2 expression levels in AD brains (n=697) compared with healthy (non-demented healthy control (NDHC)) (n=460) **(a);** High diagnostic ability of CHI3L1 (p<0.0001, AUC=0.8574) to discriminate healthy subjects from AD patients, and Satisfactory ability of CHI3L2 (p<0.0001, AUC=0.6932) **(b);** Pearson correlation analysis performed between CHI3L1 (r=0.3566, p<0.0001), and CHI3L2 (r=0.4479, p<0.0001), and astrocyte activation marker GFAP **(c);** Pearson correlation analysis performed between CHI3L1 (r=0.2845, p<0.0001), and CHI3L2 (r=0.1471, p<0.0001), and microglia marker TMEM119 **(d).** The dashed lines indicate the maximum and minimum mean values. Data are expressed as z-score intensity expression levels (means and SD) and presented as

violin dot plots. The orange dots indicate the upper and lower quartile CHI3L1 expression levels. P values <0.05 were considered as statistically significant (****p<0.00001).

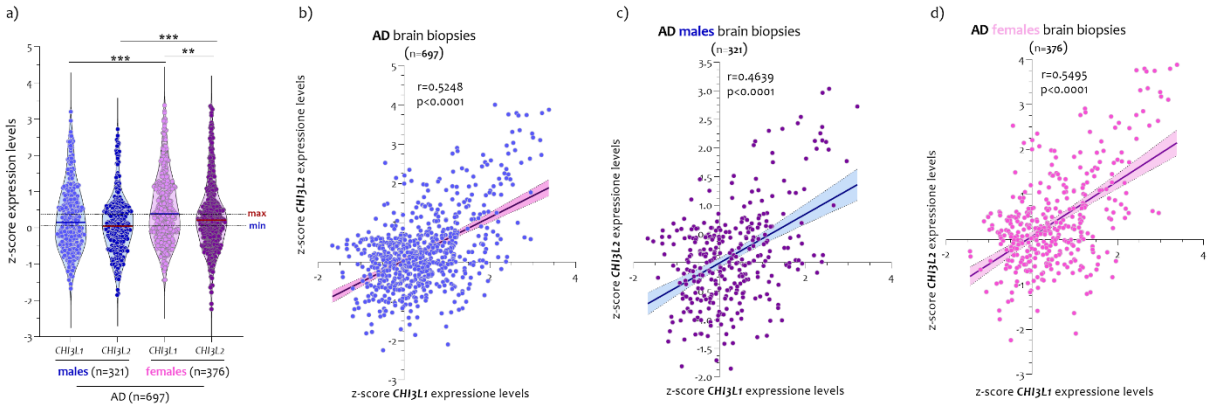

Figure 2: CHI3L1 and CHI3L2 expression and correlation analysis in AD brain biopsies according to patient's sex

Significantly higher expression of CHI3L1 and CHI3L2 in female compared with male AD **(a).** Pearson correlation analysis performed between CHI3L1 and CHI3L2 in all samples **(b)** (r=0.5248, p<0.0001), in males **(c)** (r=0.4639, p<0.0001), and in females AD **(d)** (r=0.5495, p<0.0001). The dashed lines indicate the maximum and minimum mean values. Data are expressed as z-score intensity expression levels (means and SD) and presented as dot plots. P values <0.05 were considered as statistically significant (**p<0.001, ***p<0.0001).

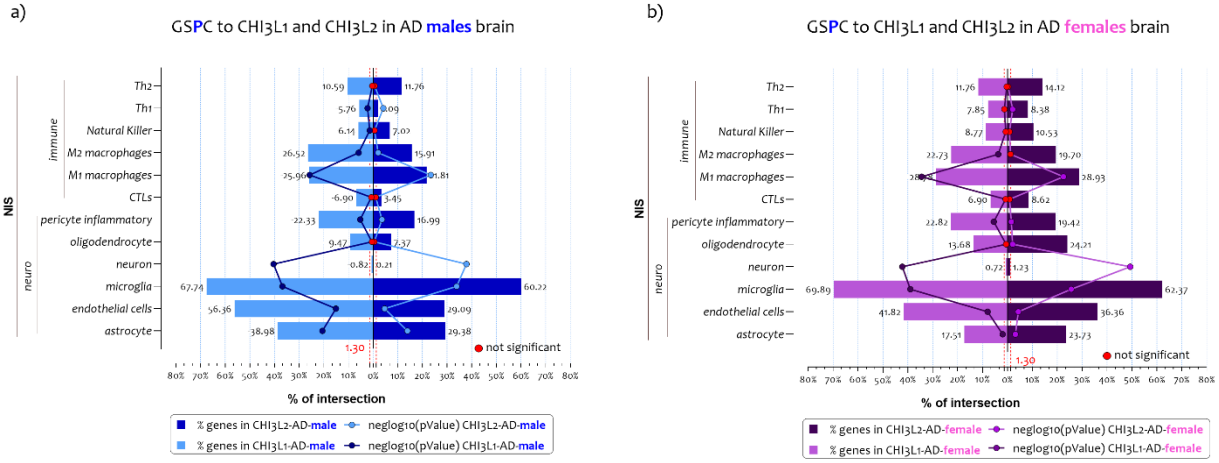

Figure 3: NIS deconvolution analysis obtained by GSPC- CHI3L1 and GSPC- CHI3L2 in AD males and female brains

Overlapping of genes positively (GSPC) correlated to CHI3L1 and CHI3L2 expression levels in brain of AD patients to twelve signatures of CNS cells and the immune cells (NIS), both in males **(a)** and females **(b).** The genes in common obtained from the overlaps are expressed in percentages and represented as bar charts. The p-value obtained by Fisher's test is expressed as $neglog_{10}$ (pvalue) and represented as lines charts. The red points represent the non-significant percentage intersections. P-values <0.05 were considered as statistically significant ($neglog_{10}$(pvalue)> 1.30).

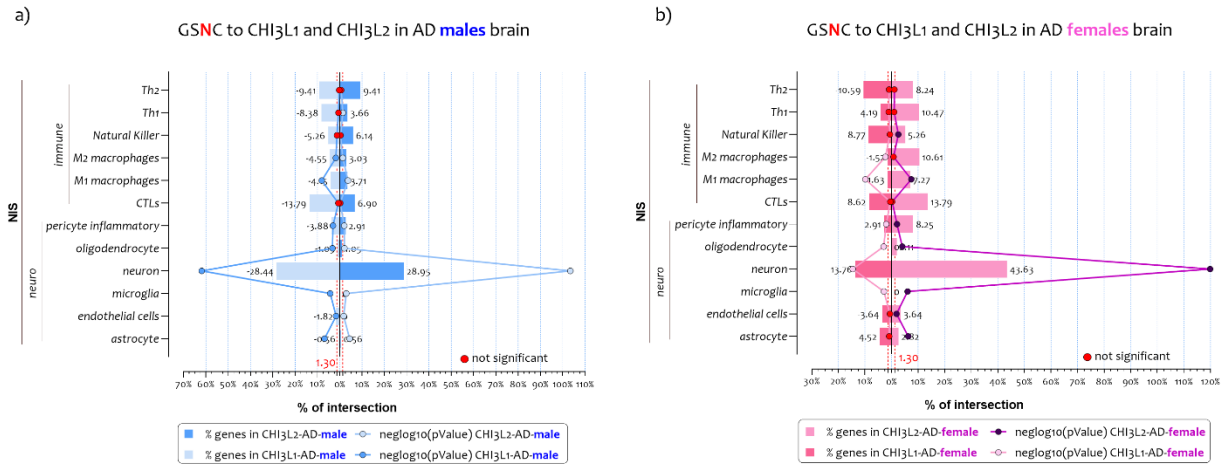

Figure 4: NIS deconvolution analysis obtained by GSNC- CHI3L1 and GSNC- CHI3L2 in AD males and female brains

Overlapping of genes negatively (GSNC) correlated to CHI3L1 and CHI3L2 expression levels in brain of AD patients to twelve signatures of CNS cells and the immune cells (NIS), both in males **(a)** and females **(b).** The genes in common obtained from the overlaps are expressed in percentages and represented as bar charts. The p-value obtained by Fisher's test is expressed as neglog10 (pvalue) and represented as lines charts. The red points represent the non-significant percentage intersections. P-values <0.05 were considered as statistically significant (neglog10(pvalue)> 1.30).

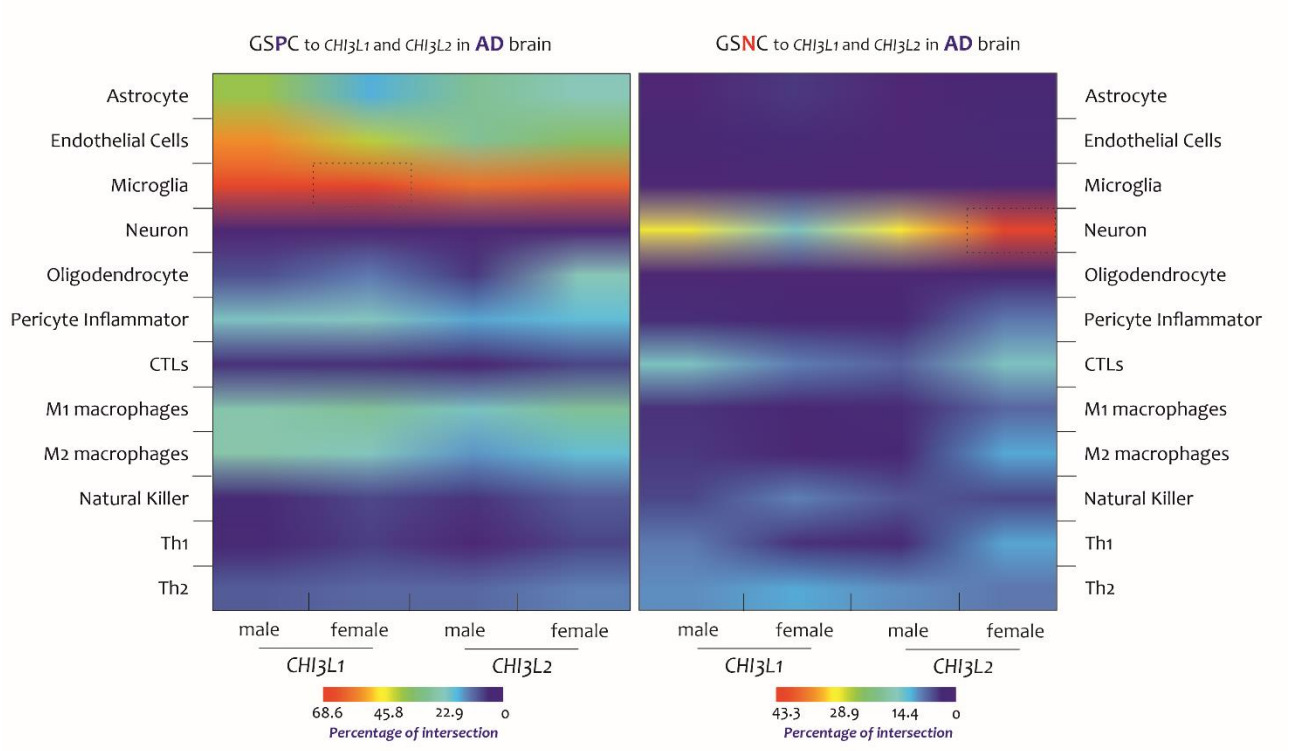

Figure 5: Heatmap NIS deconvolution

High percentage of intersections was found between the microglial profile and the GSPC2-male-female and GSPC1-male transcriptome. Regarding the microglia highlighted by GSPC-CHI3L1-female, and the neuron highlighted by GSNC-CHI3L2-female transcriptomes showed the high percentages of intersections. The gradient color (smaller values in blue and larger values in red) indicates the percentage of intersections by the GSPC/GSNC/CHI3L1/CHI3L2 to the NIS.

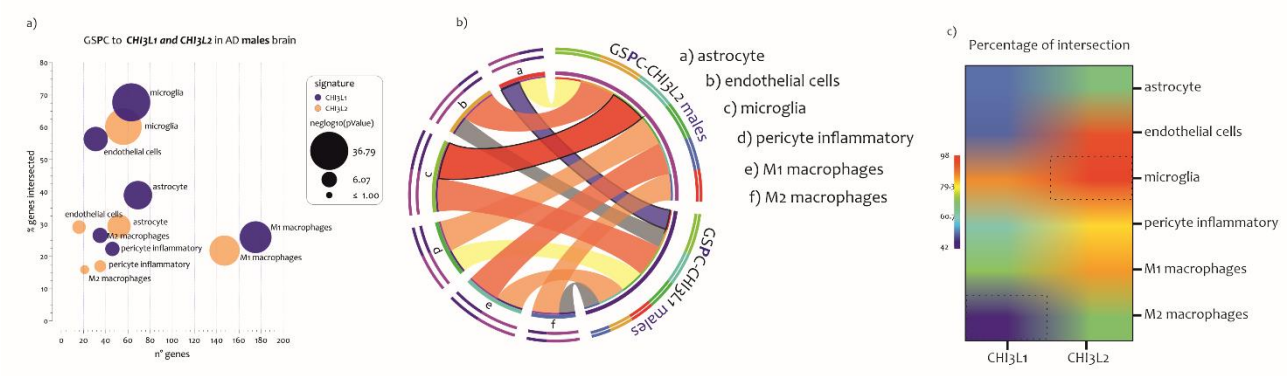

Figure 6: Signature similarity between NIS determined by GSPC-CHI3L1 and GSPC-CHI3L2 in AD males

Bubble-chart of the percentage of genes significantly involved in NIS determined by GSPC-CHI3L1 and GSPC-CHI3L2 in AD males. The different colors indicate the signatures identified by CHI3L1 and CHI3L2, while the circle's size indicates neg log10 (p-value) **(a).** Cord-diagram of microglia-NIS identified by GSPC-CHI3L1 and GSPC-CHI3L2 males. The red cord represents the highest genomic share (similarity between CHI3L1 and CHI3L2) (98.2% for microglia identified by the GSPC-CHI3L2-male signature) and the blue string the lowest (42.9% for M2 macrophages identified by the GSPC-CHI3L1-male signature) **(b).** Heat-map of signature similarity between NIS determined by GSPC-CHI3L1 and GSPC-CHI3L2 in males. The dashed boxes indicate the most regulated NIS **(c).**

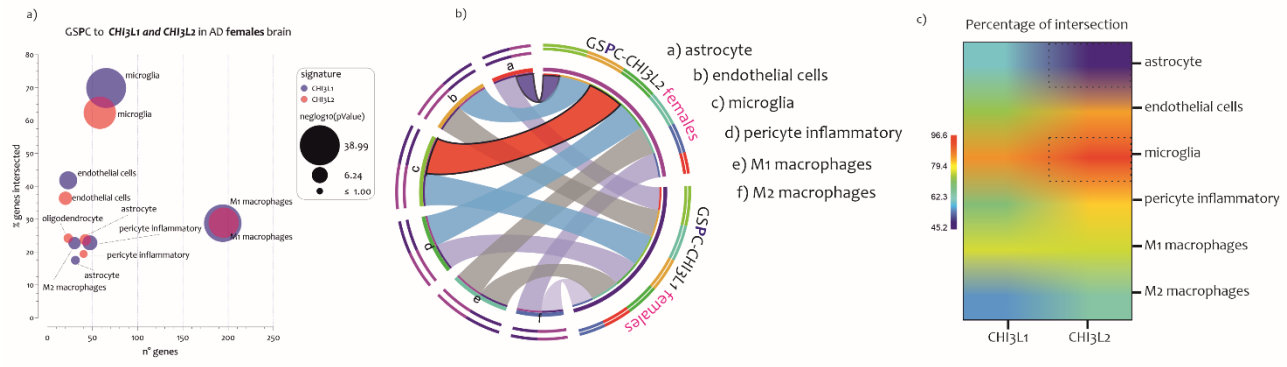

Figure 7: Signature similarity between NIS determined by GSPC-CHI3L1 and GSPC-CHI3L2 in AD females

Bubble-chart of the percentage of genes significantly involved in NIS determined by GSPC-CHI3L1 and GSPC-CHI3L2 in AD females. The different colors indicate the signatures identified by CHI3L1 and CHI3L2, while the circle's size indicates neg log10 (p-value) **(a).** Cord-diagram of microglia-NIS identified by GSPC-CHI3L1 and GSPC-CHI3L2 females. The red cord represents the highest genomic share (similarity between CHI3L1 and CHI3L2) (96.6% for microglia identified by the GSPC-CHI3L2-female signature) and the blue string the lowest (45.2% for astrocyte identified by the GSPC-CHI3L2-female signature) **(b).** Heat-map of signature similarity between NIS determined by GSPC-CHI3L1 and GSPC-CHI3L2 in females. The dashed boxes indicate the most regulated NIS **(c).**

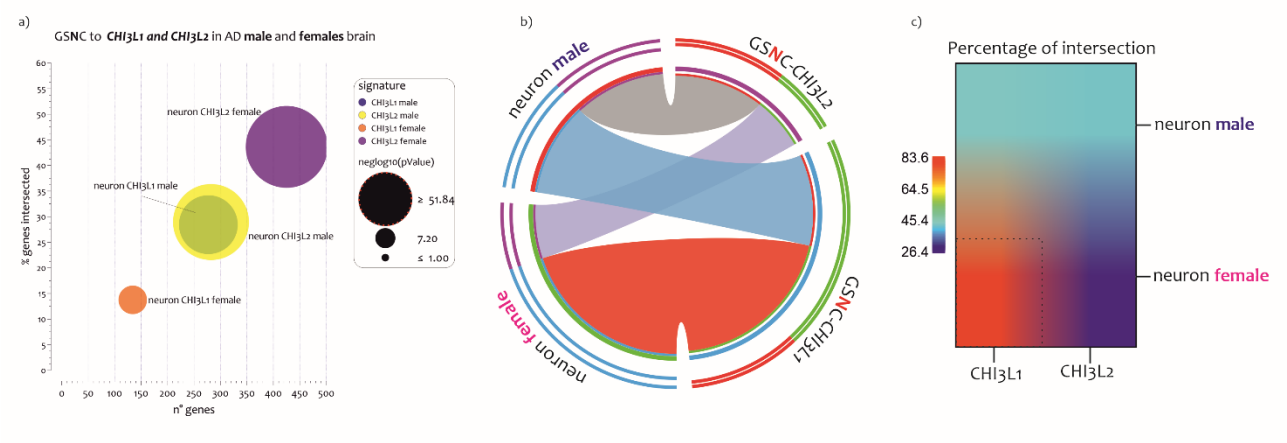

Figure 8: Signature similarity between NIS determined by GSNC-CHI3L1 and GSNC-CHI3L2 in AD males and females

Bubble-chart of the percentage of genes significantly involved in NIS determined by GSNC-CHI3L1 and GSNC-CHI3L2 in AD males and females. The different colors indicate the signatures identified by CHI3L1 and CHI3L2, while the circle's size indicates neg log10 (p-value) **(a).** Cord-diagram of microglia-NIS identified by GSNC-CHI3L1 and GSNC-CHI3L2 males and females. The red cord represents the highest genomic share (similarity between CHI3L1 and CHI3L2) (83.6% for neuron identified by the GSNC-CHI3L1-female signature) **(b).** Heat-map of signature similarity between NIS determined by GSNC-CHI3L1 and GSPC-CHI3L2 in males and females. The dashed boxes indicate the most regulated NIS **(c).**

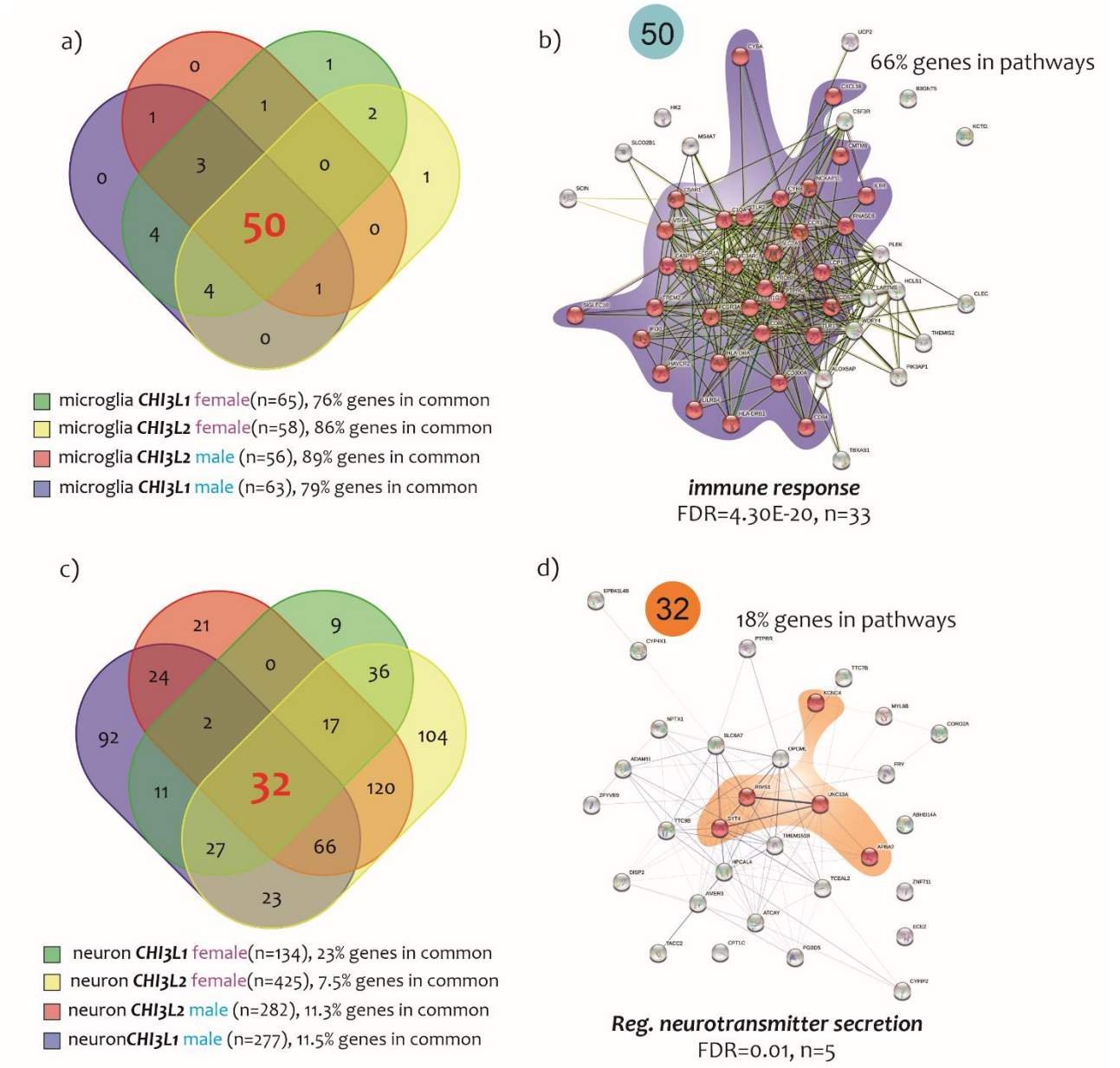

Figure 9: GO analysis of common genes identified by the microglia and neuron signatures determined by CHI3L1 and CHI3L2

Venn's analysis crossing the microglia NIS signatures obtained from GSPC-CHI3L1-male, GSPC-CHI3L1-female, GSPC-CHI3L2-male, and GSPC-CHI3L2-female. The analysis showed 50 genes in common between all microglia-NIS **(a).** GO analysis of the 50 genes in common among the microglia-NIS. The main biological process involved in activation of 50 genes was the *immune response* (FDR = 4.30E-20, n = 33) **(b).** Venn's analysis crossing the neuron NIS signatures obtained from GSNC-CHI3L1-male, GSNC-CHI3L1-female, GSNC-CHI3L2-male, and GSNC-CHI3L2-female. The analysis showed 32 genes in common between all neuron-NIS **(c).** GO analysis of the 32 genes in common among the neuron-NIS. The main biological process involved in activation of 32 genes was the *regulation of neurotransmitter secretion* (FDR = 0.001, n = 5) **(d).**

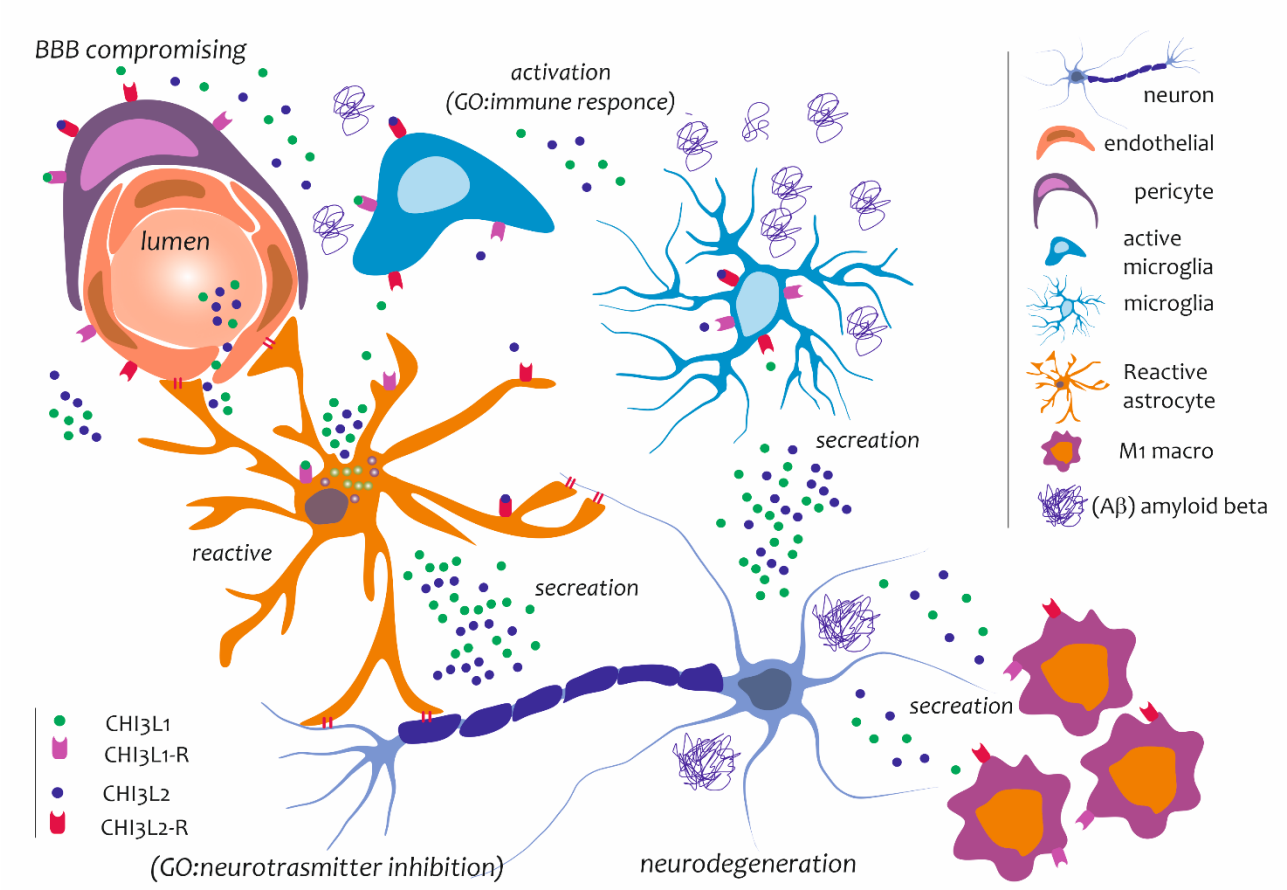

Figure 10: Potential role played by CHI3L1 and ChI3L2 in AD brain

CHI3L1 and CHI3L2 may be cytokines that mediate neuroinflammatory processes to trigger receptors expressed on target brain cells (microglia, pericytes, endothelial cells) and regulate innate inflammatory responses (M1 macrophages).

TABLES

Table 1: *Datasets selected*

Table 2: *AD patients' stratification*

Table 3: *The twelve signature – Neuro-immune signature (NIS)*

Table 4: *Signature similarity*

Supplementary Table 1: *Data analysis*

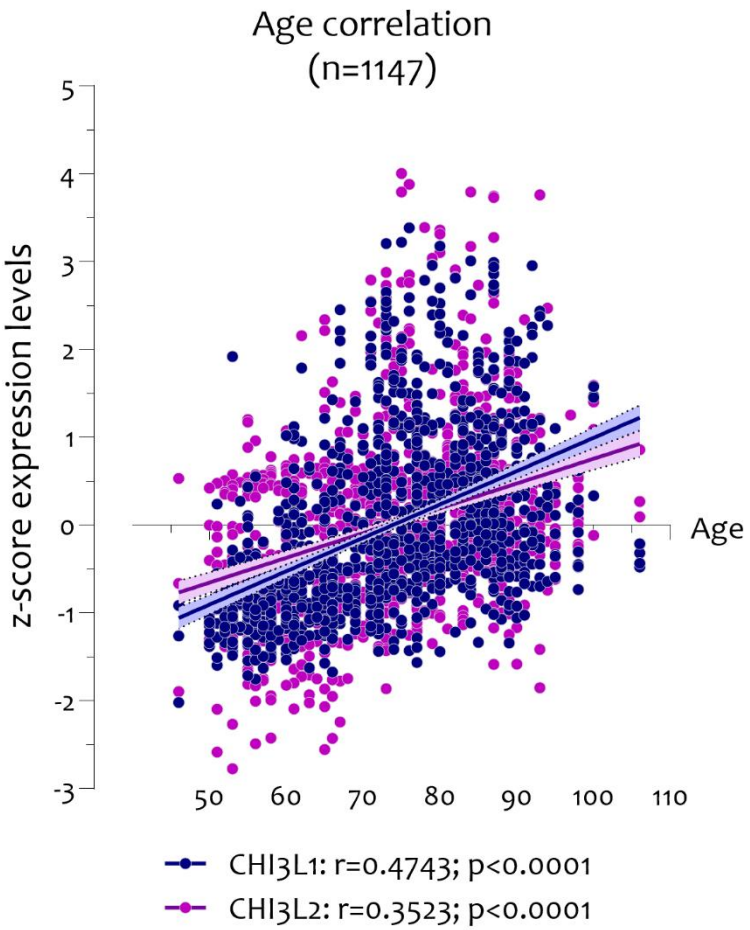

Supplementary Figure 1: *age correlation*

Reference

Abbas, A.R., Baldwin, D., Ma, Y., Ouyang, W., Gurney, A., Martin, F., Fong, S., van Lookeren Campagne, M., Godowski, P., Williams, P.M., Chan, A.C., Clark, H.F., 2005. Immune response in silico (IRIS): immune-specific genes identified from a compendium of microarray expression data. Genes Immun. 6**,** 319-31.

Abbott, N.J., 2002. Astrocyte-endothelial interactions and blood-brain barrier permeability. J Anat. 200**,** 629-38.

Alcolea, D., Carmona-Iragui, M., Suarez-Calvet, M., Sanchez-Saudinos, M.B., Sala, I., Anton-Aguirre, S., Blesa, R., Clarimon, J., Fortea, J., Lleo, A., 2014. Relationship between beta-

Secretase, inflammation and core cerebrospinal fluid biomarkers for Alzheimer's disease. J Alzheimers Dis. 42**,** 157-67.

Alcolea, D., Vilaplana, E., Pegueroles, J., Montal, V., Sanchez-Juan, P., Gonzalez-Suarez, A., Pozueta, A., Rodriguez-Rodriguez, E., Bartres-Faz, D., Vidal-Pineiro, D., Gonzalez-Ortiz, S., Medrano, S., Carmona-Iragui, M., Sanchez-Saudinos, M., Sala, I., Anton-Aguirre, S., Sampedro, F., Morenas-Rodriguez, E., Clarimon, J., Blesa, R., Lleo, A., Fortea, J., 2015. Relationship between cortical thickness and cerebrospinal fluid YKL-40 in predementia stages of Alzheimer's disease. Neurobiol Aging. 36**,** 2018-23.

Antonell, A., Mansilla, A., Rami, L., Llado, A., Iranzo, A., Olives, J., Balasa, M., Sanchez-Valle, R., Molinuevo, J.L., 2014. Cerebrospinal fluid level of YKL-40 protein in preclinical and prodromal Alzheimer's disease. J Alzheimers Dis. 42**,** 901-8.

Bonneh-Barkay, D., Bissel, S.J., Wang, G., Fish, K.N., Nicholl, G.C., Darko, S.W., Medina-Flores, R., Murphey-Corb, M., Rajakumar, P.A., Nyaundi, J., Mellors, J.W., Bowser, R., Wiley, C.A., 2008. YKL-40, a marker of simian immunodeficiency virus encephalitis, modulates the biological activity of basic fibroblast growth factor. Am J Pathol. 173**,** 130-43.

Bonneh-Barkay, D., Zagadailov, P., Zou, H., Niyonkuru, C., Figley, M., Starkey, A., Wang, G., Bissel, S.J., Wiley, C.A., Wagner, A.K., 2010. YKL-40 expression in traumatic brain injury: an initial analysis. J Neurotrauma. 27**,** 1215-23.

Bonneh-Barkay, D., Bissel, S.J., Kofler, J., Starkey, A., Wang, G., Wiley, C.A., 2012. Astrocyte and macrophage regulation of YKL-40 expression and cellular response in neuroinflammation. Brain Pathol. 22**,** 530-46.

Buchman, A.S., Boyle, P.A., Yu, L., Shah, R.C., Wilson, R.S., Bennett, D.A., 2012. Total daily physical activity and the risk of AD and cognitive decline in older adults. Neurology. 78**,** 1323-9.

Care, M.A., Barrans, S., Worrillow, L., Jack, A., Westhead, D.R., Tooze, R.M., 2013. A microarray platform-independent classification tool for cell of origin class allows comparative analysis of gene expression in diffuse large B-cell lymphoma. PLoS One. 8**,** e55895.

Carter, S.F., Herholz, K., Rosa-Neto, P., Pellerin, L., Nordberg, A., Zimmer, E.R., 2019. Astrocyte Biomarkers in Alzheimer's Disease. Trends Mol Med. 25**,** 77-95.

Castrogiovanni, P., Li Volti, G., Sanfilippo, C., Tibullo, D., Galvano, F., Vecchio, M., Avola, R., Barbagallo, I., Malaguarnera, L., Castorina, S., Musumeci, G., Imbesi, R., Di Rosa, M., 2018. Fasting and Fast Food Diet Play an Opposite Role in Mice Brain Aging. Mol Neurobiol. 55**,** 6881-6893.

Castrogiovanni, P., Sanfilippo, C., Imbesi, R., Maugeri, G., Lo Furno, D., Tibullo, D., Castorina, A., Musumeci, G., Di Rosa, M., 2021. Brain CHID1 Expression Correlates with NRGN and CALB1 in Healthy Subjects and AD Patients. Cells. 10.

Catrogiovanni, P., Musumeci, G., Giunta, S., Imbesi, R., Di Rosa, M., 2020. The expression levels of CHI3L1 and IL15Ralpha correlate with TGM2 in duodenum biopsies of patients with celiac disease. Inflamm Res. 69**,** 925-935.

Chang, J.T., Nevins, J.R., 2006. GATHER: a systems approach to interpreting genomic signatures. Bioinformatics. 22**,** 2926-33.

Cheadle, C., Cho-Chung, Y.S., Becker, K.G., Vawter, M.P., 2003a. Application of z-score transformation to Affymetrix data. Appl Bioinformatics. 2**,** 209-17.

Cheadle, C., Vawter, M.P., Freed, W.J., Becker, K.G., 2003b. Analysis of microarray data using Z score transformation. The Journal of molecular diagnostics : JMD. 5**,** 73-81.

Chen, Q.R., Song, Y.K., Wei, J.S., Bilke, S., Asgharzadeh, S., Seeger, R.C., Khan, J., 2008. An integrated cross-platform prognosis study on neuroblastoma patients. Genomics. 92**,** 195-203.

Chen, Y., Hong, T., Chen, F., Sun, Y., Wang, Y., Cui, L., 2021. Interplay Between Microglia and Alzheimer's Disease-Focus on the Most Relevant Risks: APOE Genotype, Sex and Age. Front Aging Neurosci. 13**,** 631827.

Choi, J., Lee, H.W., Suk, K., 2011. Plasma level of chitinase 3-like 1 protein increases in patients with early Alzheimer's disease. J Neurol. 258**,** 2181-5.

Clarke, L.E., Liddelow, S.A., Chakraborty, C., Munch, A.E., Heiman, M., Barres, B.A., 2018. Normal aging induces A1-like astrocyte reactivity. Proc Natl Acad Sci U S A. 115**,** E1896-E1905.

Colombo, E., Farina, C., 2016. Astrocytes: Key Regulators of Neuroinflammation. Trends Immunol. 37**,** 608-620.

Connolly, K., Lehoux, M., O'Rourke, R., Assetta, B., Erdemir, G.A., Elias, J.A., Lee, C.G., Huang, Y.A., 2022. Potential role of chitinase-3-like protein 1 (CHI3L1/YKL-40) in neurodegeneration and Alzheimer's disease. Alzheimers Dement.

Craig-Schapiro, R., Perrin, R.J., Roe, C.M., Xiong, C., Carter, D., Cairns, N.J., Mintun, M.A., Peskind, E.R., Li, G., Galasko, D.R., Clark, C.M., Quinn, J.F., D'Angelo, G., Malone, J.P., Townsend, R.R., Morris, J.C., Fagan, A.M., Holtzman, D.M., 2010. YKL-40: a novel prognostic fluid biomarker for preclinical Alzheimer's disease. Biol Psychiatry. 68**,** 903-12.

Cunningham, C., Wilcockson, D.C., Campion, S., Lunnon, K., Perry, V.H., 2005. Central and systemic endotoxin challenges exacerbate the local inflammatory response and increase neuronal death during chronic neurodegeneration. J Neurosci. 25**,** 9275-84.

Davis, S., Meltzer, P.S., 2007. GEOquery: a bridge between the Gene Expression Omnibus (GEO) and BioConductor. Bioinformatics. 23**,** 1846-7.

Di Rosa, M., Dell'Ombra, N., Zambito, A.M., Malaguarnera, M., Nicoletti, F., Malaguarnera, L., 2006. Chitotriosidase and inflammatory mediator levels in Alzheimer's disease and cerebrovascular dementia. Eur J Neurosci. 23**,** 2648-56.

Di Rosa, M., Zambito, A.M., Marsullo, A.R., Li Volti, G., Malaguarnera, L., 2009. Prolactin induces chitotriosidase expression in human macrophages through PTK, PI3-K, and MAPK pathways. J Cell Biochem. 107**,** 881-9.

Di Rosa, M., Malaguarnera, G., De Gregorio, C., Drago, F., Malaguarnera, L., 2013. Evaluation of CHI3L-1 and CHIT-1 expression in differentiated and polarized macrophages. Inflammation. 36**,** 482-92.

Di Rosa, M., Szychlinska, M.A., Tibullo, D., Malaguarnera, L., Musumeci, G., 2014a. Expression of CHI3L1 and CHIT1 in osteoarthritic rat cartilage model. A morphological study. Eur J Histochem. 58**,** 2423.

Di Rosa, M., Tibullo, D., Vecchio, M., Nunnari, G., Saccone, S., Di Raimondo, F., Malaguarnera, L., 2014b. Determination of chitinases family during osteoclastogenesis. Bone. 61**,** 55-63.

Di Rosa, M., Sanfilippo, C., Libra, M., Musumeci, G., Malaguarnera, L., 2015. Different pediatric brain tumors are associated with different gene expression profiling. Acta Histochem. 117**,** 477-85.

Di Rosa, M., Distefano, G., Zorena, K., Malaguarnera, L., 2016a. Chitinases and immunity: Ancestral molecules with new functions. Immunobiology. 221**,** 399-411.

Di Rosa, M., Malaguarnera, L., 2016. Chitinase 3 Like-1: An Emerging Molecule Involved in Diabetes and Diabetic Complications. Pathobiology. 83**,** 228-42.

Di Rosa, M., Tibullo, D., Saccone, S., Distefano, G., Basile, M.S., Di Raimondo, F., Malaguarnera, L., 2016b. CHI3L1 nuclear localization in monocyte derived dendritic cells. Immunobiology. 221**,** 347-56.

Di Rosa, M., Giallongo, C., Romano, A., Tibullo, D., Li Volti, G., Musumeci, G., Barbagallo, I., Imbesi, R., Castrogiovanni, P., Palumbo, G.A., 2020. Immunoproteasome Genes Are Modulated in CD34(+) JAK2(V617F) Mutated Cells from Primary Myelofibrosis Patients. Int J Mol Sci. 21.

Eide, K.B., Stockinger, L.W., Lewin, A.S., Tondervik, A., Eijsink, V.G., Sorlie, M., 2016. The role of active site aromatic residues in substrate degradation by the human chitotriosidase. Biochim Biophys Acta. 1864**,** 242-7.

El Khoury, J.B., Moore, K.J., Means, T.K., Leung, J., Terada, K., Toft, M., Freeman, M.W., Luster, A.D., 2003. CD36 mediates the innate host response to beta-amyloid. J Exp Med. 197**,** 1657-66.

Feng, C., Wu, J., Yang, F., Qiu, M., Hu, S., Guo, S., Wu, J., Ying, X., Wang, J., 2018. Expression of Bcl-2 is a favorable prognostic biomarker in lung squamous cell carcinoma. Oncol Lett. 15**,** 6925-6930.

Giunta, S., Castorina, A., Marzagalli, R., Szychlinska, M.A., Pichler, K., Mobasheri, A., Musumeci, G., 2015. Ameliorative effects of PACAP against cartilage degeneration. Morphological, immunohistochemical and biochemical evidence from in vivo and in vitro models of rat osteoarthritis. Int J Mol Sci. 16**,** 5922-44.

Glenner, G.G., Wong, C.W., 1984. Alzheimer's disease: initial report of the purification and characterization of a novel cerebrovascular amyloid protein. Biochem Biophys Res Commun. 120**,** 885-90.

Grundke-Iqbal, I., Iqbal, K., Tung, Y.C., Quinlan, M., Wisniewski, H.M., Binder, L.I., 1986. Abnormal phosphorylation of the microtubule-associated protein tau (tau) in Alzheimer cytoskeletal pathology. Proc Natl Acad Sci U S A. 83**,** 4913-7.

Guijarro-Munoz, I., Compte, M., Alvarez-Cienfuegos, A., Alvarez-Vallina, L., Sanz, L., 2014. Lipopolysaccharide activates Toll-like receptor 4 (TLR4)-mediated NF-kappaB signaling pathway and proinflammatory response in human pericytes. J Biol Chem. 289**,** 2457-68.

Gurwitz, D., 1997. Auguste D and Alzheimer's disease. Lancet. 350**,** 298.

Harris, V.K., Sadiq, S.A., 2014. Biomarkers of therapeutic response in multiple sclerosis: current status. Mol Diagn Ther. 18**,** 605-17.

Henrissat, B., Davies, G., 1997. Structural and sequence-based classification of glycoside hydrolases. Curr Opin Struct Biol. 7**,** 637-44.

Heppner, F.L., Ransohoff, R.M., Becher, B., 2015. Immune attack: the role of inflammation in Alzheimer disease. Nat Rev Neurosci. 16**,** 358-72.

Hillman, C.H., Erickson, K.I., Kramer, A.F., 2008. Be smart, exercise your heart: exercise effects on brain and cognition. Nat Rev Neurosci. 9**,** 58-65.

Hong, S., Dobricic, V., Ohlei, O., Bos, I., Vos, S.J.B., Prokopenko, D., Tijms, B.M., Andreasson, U., Blennow, K., Vandenberghe, R., Gabel, S., Scheltens, P., Teunissen, C.E., Engelborghs, S., Frisoni, G., Blin, O., Richardson, J.C., Bordet, R., Alzheimer's Disease Neuroimaging, I., Lleo, A., Alcolea, D., Popp, J., Clark, C., Peyratout, G., Martinez-Lage, P., Tainta, M., Dobson, R.J.B., Legido-Quigley, C., Sleegers, K., Van Broeckhoven, C., Tanzi, R.E., Ten Kate, M., Wittig, M., Franke, A., Lill, C.M., Barkhof, F., Lovestone, S., Streffer, J., Zetterberg, H., Visser, P.J., Bertram, L., 2021. TMEM106B and CPOX are genetic determinants of cerebrospinal fluid Alzheimer's disease biomarker levels. Alzheimers Dement. 17**,** 1628-1640.

Kanegawa, N., Collste, K., Forsberg, A., Schain, M., Arakawa, R., Jucaite, A., Lekander, M., Olgart Hoglund, C., Kosek, E., Lampa, J., Halldin, C., Farde, L., Varrone, A., Cervenka, S., 2016. In vivo evidence of a functional association between immune cells in blood and brain in healthy human subjects. Brain Behav Immun. 54**,** 149-157.

Kang, C., Huo, Y., Xin, L., Tian, B., Yu, B., 2019. Feature selection and tumor classification for microarray data using relaxed Lasso and generalized multi-class support vector machine. J Theor Biol. 463**,** 77-91.

Kenkhuis, B., Somarakis, A., Kleindouwel, L.R.T., van Roon-Mom, W.M.C., Hollt, T., van der Weerd, L., 2022. Co-expression patterns of microglia markers Iba1, TMEM119 and P2RY12 in Alzheimer's disease. Neurobiol Dis. 167**,** 105684.

Kwak, E.J., Hong, J.Y., Kim, M.N., Kim, S.Y., Kim, S.H., Park, C.O., Kim, K.W., Lee, C.G., Elias, J.A., Jee, H.M., Sohn, M.H., 2019. Chitinase 3-like 1 drives allergic skin inflammation via Th2 immunity and M2 macrophage activation. Clin Exp Allergy. 49**,** 1464-1474.

Lawson, L.J., Perry, V.H., Dri, P., Gordon, S., 1990. Heterogeneity in the distribution and morphology of microglia in the normal adult mouse brain. Neuroscience. 39**,** 151-70.

Le Cao, K.A., Rohart, F., McHugh, L., Korn, O., Wells, C.A., 2014. YuGene: a simple approach to scale gene expression data derived from different platforms for integrated analyses. Genomics. 103**,** 239-51.

Lee, C.G., Da Silva, C.A., Dela Cruz, C.S., Ahangari, F., Ma, B., Kang, M.J., He, C.H., Takyar, S., Elias, J.A., 2011. Role of chitin and chitinase/chitinase-like proteins in inflammation, tissue remodeling, and injury. Annu Rev Physiol. 73**,** 479-501.

Liddelow, S.A., Barres, B.A., 2017. Reactive Astrocytes: Production, Function, and Therapeutic Potential. Immunity. 46**,** 957-967.

Litviakov, N., Tsyganov, M., Larionova, I., Ibragimova, M., Deryusheva, I., Kazantseva, P., Slonimskaya, E., Frolova, I., Choinzonov, E., Cherdyntseva, N., Kzhyshkowska, J., 2018. Expression of M2 macrophage markers YKL-39 and CCL18 in breast cancer is associated with the effect of neoadjuvant chemotherapy. Cancer Chemother Pharmacol. 82**,** 99-109.

Lomiguen, C., Vidal, L., Kozlowski, P., Prancan, A., Stern, R., 2018. Possible Role of Chitin-Like Proteins in the Etiology of Alzheimer's Disease. J Alzheimers Dis. 66**,** 439-444.

Malaguarnera, L., Imbesi, R., Di Rosa, M., Scuto, A., Castrogiovanni, P., Messina, A., Sanfilippo, S., 2005. Action of prolactin, IFN-gamma, TNF-alpha and LPS on heme oxygenase-1 expression and VEGF release in human monocytes/macrophages. Int Immunopharmacol. 5**,** 1458-69.

Malaguarnera, L., Motta, M., Di Rosa, M., Anzaldi, M., Malaguarnera, M., 2006. Interleukin-18 and transforming growth factor-beta 1 plasma levels in Alzheimer's disease and vascular dementia. Neuropathology. 26**,** 307-12.

Mayeux, R., Stern, Y., 2012. Epidemiology of Alzheimer disease. Cold Spring Harb Perspect Med. 2.

Medeiros, R., LaFerla, F.M., 2013. Astrocytes: conductors of the Alzheimer disease neuroinflammatory symphony. Exp Neurol. 239**,** 133-8.

Mehmood, R., El-Ashram, S., Bie, R., Dawood, H., Kos, A., 2017. Clustering by fast search and merge of local density peaks for gene expression microarray data. Sci Rep. 7**,** 45602.

Melah, K.E., Lu, S.Y., Hoscheidt, S.M., Alexander, A.L., Adluru, N., Destiche, D.J., Carlsson, C.M., Zetterberg, H., Blennow, K., Okonkwo, O.C., Gleason, C.E., Dowling, N.M., Bratzke, L.C., Rowley, H.A., Sager, M.A., Asthana, S., Johnson, S.C., Bendlin, B.B., 2016. Cerebrospinal Fluid Markers of Alzheimer's Disease Pathology and Microglial Activation are Associated with Altered White Matter Microstructure in Asymptomatic Adults at Risk for Alzheimer's Disease. J Alzheimers Dis. 50**,** 873-86.

Mollgaard, M., Degn, M., Sellebjerg, F., Frederiksen, J.L., Modvig, S., 2016. Cerebrospinal fluid chitinase-3-like 2 and chitotriosidase are potential prognostic biomarkers in early multiple sclerosis. Eur J Neurol. 23**,** 898-905.

Moreno-Rodriguez, M., Perez, S.E., Nadeem, M., Malek-Ahmadi, M., Mufson, E.J., 2020. Frontal cortex chitinase and pentraxin neuroinflammatory alterations during the progression of Alzheimer's disease. J Neuroinflammation. 17**,** 58.

Motta, M., Imbesi, R., Di Rosa, M., Stivala, F., Malaguarnera, L., 2007. Altered plasma cytokine levels in Alzheimer's disease: correlation with the disease progression. Immunol Lett. 114**,** 46-51.

Nagele, R.G., D'Andrea, M.R., Lee, H., Venkataraman, V., Wang, H.Y., 2003. Astrocytes accumulate A beta 42 and give rise to astrocytic amyloid plaques in Alzheimer disease brains. Brain Res. 971**,** 197-209.

Olsson, B., Malmestrom, C., Basun, H., Annas, P., Hoglund, K., Lannfelt, L., Andreasen, N., Zetterberg, H., Blennow, K., 2012. Extreme stability of chitotriosidase in cerebrospinal fluid makes it a suitable marker for microglial activation in clinical trials. J Alzheimers Dis. 32**,** 273-6.

Plassman, B.L., Langa, K.M., Fisher, G.G., Heeringa, S.G., Weir, D.R., Ofstedal, M.B., Burke, J.R., Hurd, M.D., Potter, G.G., Rodgers, W.L., Steffens, D.C., Willis, R.J., Wallace, R.B., 2007. Prevalence of dementia in the United States: the aging, demographics, and memory study. Neuroepidemiology. 29**,** 125-32.

Qiu, Q.C., Wang, L., Jin, S.S., Liu, G.F., Liu, J., Ma, L., Mao, R.F., Ma, Y.Y., Zhao, N., Chen, M., Lin, B.Y., 2018. CHI3L1 promotes tumor progression by activating TGF-beta signaling pathway in hepatocellular carcinoma. Sci Rep. 8**,** 15029.

Querol-Vilaseca, M., Colom-Cadena, M., Pegueroles, J., San Martin-Paniello, C., Clarimon, J., Belbin, O., Fortea, J., Lleo, A., 2017. YKL-40 (Chitinase 3-like I) is expressed in a subset of astrocytes in Alzheimer's disease and other tauopathies. J Neuroinflammation. 14**,** 118.

Reddy, T.B., Riley, R., Wymore, F., Montgomery, P., DeCaprio, D., Engels, R., Gellesch, M., Hubble, J., Jen, D., Jin, H., Koehrsen, M., Larson, L., Mao, M., Nitzberg, M., Sisk, P., Stolte, C., Weiner, B., White, J., Zachariah, Z.K., Sherlock, G., Galagan, J.E., Ball, C.A., Schoolnik, G.K., 2009. TB database: an integrated platform for tuberculosis research. Nucleic Acids Res. 37**,** D499-508.

Rehli, M., Niller, H.H., Ammon, C., Langmann, S., Schwarzfischer, L., Andreesen, R., Krause, S.W., 2003. Transcriptional regulation of CHI3L1, a marker gene for late stages of macrophage differentiation. J Biol Chem. 278**,** 44058-67.

Rosen, C., Andersson, C.H., Andreasson, U., Molinuevo, J.L., Bjerke, M., Rami, L., Llado, A., Blennow, K., Zetterberg, H., 2014. Increased Levels of Chitotriosidase and YKL-40 in Cerebrospinal Fluid from Patients with Alzheimer's Disease. Dement Geriatr Cogn Dis Extra. 4**,** 297-304.

Sanfilippo, C., Malaguarnera, L., Di Rosa, M., 2016. Chitinase expression in Alzheimer's disease and non-demented brains regions. J Neurol Sci. 369**,** 242-249.

Sanfilippo, C., Longo, A., Lazzara, F., Cambria, D., Distefano, G., Palumbo, M., Cantarella, A., Malaguarnera, L., Di Rosa, M., 2017a. CHI3L1 and CHI3L2 overexpression in motor cortex and spinal cord of sALS patients. Mol Cell Neurosci. 85**,** 162-169.

Sanfilippo, C., Nunnari, G., Calcagno, A., Malaguarnera, L., Blennow, K., Zetterberg, H., Di Rosa, M., 2017b. The chitinases expression is related to Simian Immunodeficiency Virus Encephalitis (SIVE) and in HIV encephalitis (HIVE). Virus Res. 227**,** 220-230.

Sanfilippo, C., Pinzone, M.R., Cambria, D., Longo, A., Palumbo, M., Di Marco, R., Condorelli, F., Nunnari, G., Malaguarnera, L., Di Rosa, M., 2018. OAS Gene Family Expression Is Associated with HIV-Related Neurocognitive Disorders. Mol Neurobiol. 55**,** 1905-1914.

Sanfilippo, C., Castrogiovanni, P., Imbesi, R., Kazakowa, M., Musumeci, G., Blennow, K., Zetterberg, H., Di Rosa, M., 2019a. Sex difference in CHI3L1 expression levels in human brain aging and in Alzheimer's disease. Brain Res. 1720**,** 146305.

Sanfilippo, C., Castrogiovanni, P., Imbesi, R., Tibullo, D., Li Volti, G., Barbagallo, I., Vicario, N., Musumeci, G., Di Rosa, M., 2019b. Middle-aged healthy women and Alzheimer's disease patients present an overlapping of brain cell transcriptional profile. Neuroscience. 406**,** 333-344.

Sanfilippo, C., Castrogiovanni, P., Imbesi, R., Di Rosa, M., 2020a. CHI3L2 Expression Levels Are Correlated with AIF1, PECAM1, and CALB1 in the Brains of Alzheimer's Disease Patients. J Mol Neurosci. 70**,** 1598-1610.

Sanfilippo, C., Castrogiovanni, P., Imbesi, R., Nunnari, G., Di Rosa, M., 2020b. Postsynaptic damage and microglial activation in AD patients could be linked CXCR4/CXCL12 expression levels. Brain Res. 1749**,** 147127.

Satoh, J., Kino, Y., Asahina, N., Takitani, M., Miyoshi, J., Ishida, T., Saito, Y., 2016. TMEM119 marks a subset of microglia in the human brain. Neuropathology. 36**,** 39-49.

Schain, M., Kreisl, W.C., 2017. Neuroinflammation in Neurodegenerative Disorders-a Review. Curr Neurol Neurosci Rep. 17**,** 25.

Smyth, G.K., 2004. Linear models and empirical bayes methods for assessing differential expression in microarray experiments. Stat Appl Genet Mol Biol. 3**,** Article3.

Solito, E., Sastre, M., 2012. Microglia function in Alzheimer's disease. Front Pharmacol. 3**,** 14.

Steardo, L., Jr., Bronzuoli, M.R., Iacomino, A., Esposito, G., Steardo, L., Scuderi, C., 2015. Does neuroinflammation turn on the flame in Alzheimer's disease? Focus on astrocytes. Front Neurosci. 9**,** 259.

Szklarczyk, D., Gable, A.L., Lyon, D., Junge, A., Wyder, S., Huerta-Cepas, J., Simonovic, M., Doncheva, N.T., Morris, J.H., Bork, P., Jensen, L.J., Mering, C.V., 2019. STRING v11: protein-protein association networks with increased coverage, supporting functional discovery in genome-wide experimental datasets. Nucleic Acids Res. 47**,** D607-D613.

Szychlinska, M.A., Trovato, F.M., Di Rosa, M., Malaguarnera, L., Puzzo, L., Leonardi, R., Castrogiovanni, P., Musumeci, G., 2016. Co-Expression and Co-Localization of Cartilage Glycoproteins CHI3L1 and Lubricin in Osteoarthritic Cartilage: Morphological, Immunohistochemical and Gene Expression Profiles. Int J Mol Sci. 17**,** 359.

Teitsdottir, U.D., Halldorsson, S., Rolfsson, O., Lund, S.H., Jonsdottir, M.K., Snaedal, J., Petersen, P.H., 2021. Cerebrospinal Fluid C18 Ceramide Associates with Markers of Alzheimer's Disease and Inflammation at the Pre- and Early Stages of Dementia. J Alzheimers Dis. 81**,** 231-244.

Tiao, G.E.P.B.G.C., 6 April 1992. Bayesian Inference in Statistical Analysis.

Varghese, A.M., Sharma, A., Mishra, P., Vijayalakshmi, K., Harsha, H.C., Sathyaprabha, T.N., Bharath, S.M., Nalini, A., Alladi, P.A., Raju, T.R., 2013. Chitotriosidase - a putative biomarker for sporadic amyotrophic lateral sclerosis. Clin Proteomics. 10**,** 19.

Vina, J., Lloret, A., 2010. Why women have more Alzheimer's disease than men: gender and mitochondrial toxicity of amyloid-beta peptide. J Alzheimers Dis. 20 Suppl 2**,** S527-33.

Wang, J., Coombes, K.R., Highsmith, W.E., Keating, M.J., Abruzzo, L.V., 2004. Differences in gene expression between B-cell chronic lymphocytic leukemia and normal B cells: a meta-analysis of three microarray studies. Bioinformatics. 20**,** 3166-78.

Wang, M., Roussos, P., McKenzie, A., Zhou, X., Kajiwara, Y., Brennand, K.J., De Luca, G.C., Crary, J.F., Casaccia, P., Buxbaum, J.D., Ehrlich, M., Gandy, S., Goate, A., Katsel, P., Schadt, E., Haroutunian, V., Zhang, B., 2016. Integrative network analysis of nineteen brain regions identifies molecular signatures and networks underlying selective regional vulnerability to Alzheimer's disease. Genome Med. 8**,** 104.

Wang, W.Y., Tan, M.S., Yu, J.T., Tan, L., 2015. Role of pro-inflammatory cytokines released from microglia in Alzheimer's disease. Ann Transl Med. 3**,** 136.

Wurm, J., Behringer, S.P., Ravi, V.M., Joseph, K., Neidert, N., Maier, J.P., Doria-Medina, R., Follo, M., Delev, D., Pfeifer, D., Beck, J., Sankowski, R., Schnell, O., Heiland, D.H., 2019. Astrogliosis Releases Pro-Oncogenic Chitinase 3-Like 1 Causing MAPK Signaling in Glioblastoma. Cancers (Basel). 11.

Wyss-Coray, T., Rogers, J., 2012. Inflammation in Alzheimer disease-a brief review of the basic science and clinical literature. Cold Spring Harb Perspect Med. 2**,** a006346.

Xiao, J., Cao, H., Chen, J., 2017. False discovery rate control incorporating phylogenetic tree increases detection power in microbiome-wide multiple testing. Bioinformatics. 33**,** 2873-2881.

Yasrebi, H., Sperisen, P., Praz, V., Bucher, P., 2009. Can survival prediction be improved by merging gene expression data sets? PLoS One. 4**,** e7431.

Zetterberg, H., Bozzetta, E., Favole, A., Corona, C., Cavarretta, M.C., Ingravalle, F., Blennow, K., Pocchiari, M., Meloni, D., 2019. Neurofilaments in blood is a new promising preclinical biomarker for the screening of natural scrapie in sheep. PLoS One. 14**,** e0226697.

Zhang, Z., Ma, Z., Zou, W., Guo, H., Liu, M., Ma, Y., Zhang, L., 2019. The Appropriate Marker for Astrocytes: Comparing the Distribution and Expression of Three Astrocytic Markers in Different Mouse Cerebral Regions. Biomed Res Int. 2019**,** 9605265.

Zuberi, K., Franz, M., Rodriguez, H., Montojo, J., Lopes, C.T., Bader, G.D., Morris, Q., 2013. GeneMANIA prediction server 2013 update. Nucleic Acids Res. 41**,** W115-22.